BEILSTEIN JOURNAL OF ORGANIC CHEMISTRY

Recent advances in the synthesis of boron-stereogenic compounds

Yongke Wang[1], Sichao Tian[*1] and Weidong Zhang[*1,2]

Review

Open Access

Address:
[1]State Key Laboratory for Quality Ensurance and Sustainable Use of Dao-di Herbs, Institute of Medicinal Plant Development, Chinese Academy of Medical Sciences & Peking Union Medical College, Beijing 100193, China and [2]Department of Phytochemistry, School of Pharmacy, Second Military Medical University (Naval Medical University), Shanghai 200433, China

Email:
Sichao Tian[*] - sctian@implad.ac.cn; Weidong Zhang[*] - wdzhang@implad.ac.cn

* Corresponding author

Keywords:
asymmetric catalytic synthesis; boron-centered chirality; tetracoordinated boron compounds

Beilstein J. Org. Chem. **2026,** *22,* 1715–1739.
https://doi.org/10.3762/bjoc.22.139

Received: 28 August 2026
Accepted: 29 October 2026
Published: 19 November 2026

Associate Editor: D. Y.-K. Chen

© 2026 Wang et al.; licensee Beilstein-Institut.
License and terms: see end of document.

Abstract

Tetracoordinate boron species represent a vital class of compounds in organoboron chemistry. Owing to their unique structural features and outstanding optoelectronic properties, they exhibit broad application potential in chemical synthesis, biomedicine, and materials engineering. However, systematic synthetic protocols for chiral tetracoordinate boron complexes remain scarce. Herein, we review recent advances in the construction of stereogenic tetracoordinate boron centers, organizing catalytic approaches into six classes according to the catalyst type: copper, palladium, rhodium, nickel/cobalt, organocatalysis, and phase-transfer catalysis. The transformations covered include desymmetrization, kinetic resolution, direct asymmetric B(sp^2)-to-B(sp^3) conversion, and chirality transfer. This overview aims to inspire further development of efficient routes to chiral tetracoordinate boron compounds.

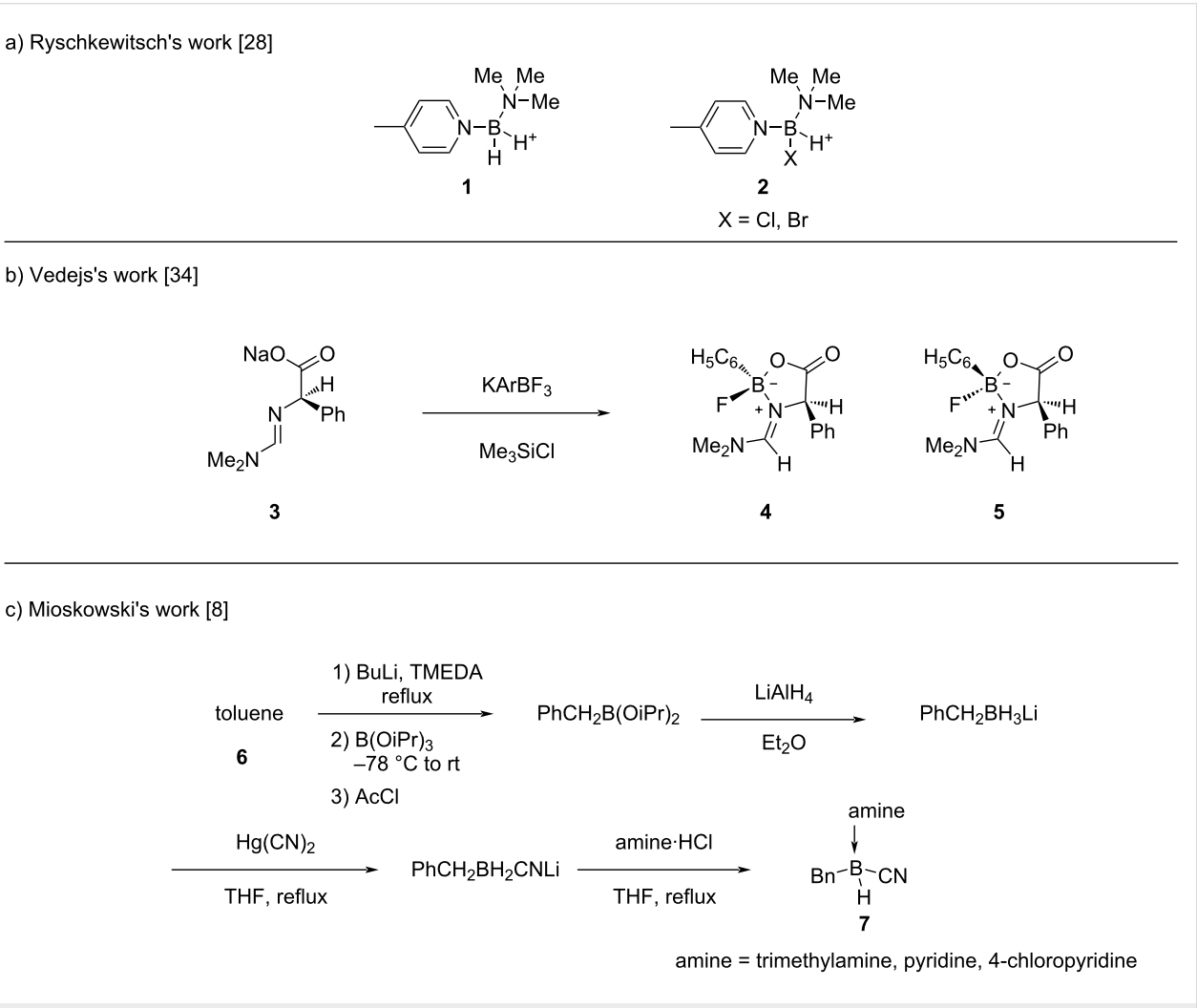
Introduction

Boron is one of the primary elements in group 13 of the periodic table. It possesses three valence electrons and typically adopts sp^2 hybridization. The boron atom bears a vacant p orbital and lone electron pairs of Lewis bases with heteroatoms such as nitrogen and oxygen can donate electron density into this orbital to form coordinate bonds, rendering boron tetracoordinate. Analogous to other stereogenic centers, a tetracoordinate boron atom functions as a chiral center when bound to four distinct substituents [1]. Nevertheless, the enantioselective synthesis of boron-stereogenic compounds remains in its infancy. One contributing factor is that ligand dissociation and stereochemical inversion proceed readily. The boron-bound ligands exhibit weak binding affinity, so the stereoconfiguration of such species is prone to scrambling. This poses a major obstacle to the rational design and preparation of tetracoordinate chiral boron species with configurationally stable stereocenters [2-7].

On the basis of established synthetic strategies, all reported routes toward boron-stereogenic compounds fall into three categories: 1) separation of chiral boron-centered species via recrystallization or high-performance liquid chromatography (HPLC) [8-15]; 2) construction of boron-centered chirality via chiral substrate induction [16-27]; 3) assembly of boron-stereogenic stereocenters through asymmetric catalysis [3,5-7].

Since the 1960s, roughly twenty research groups have investigated boron stereochemistry. Early synthetic access to boron stereoisomers rested largely on either HPLC-mediated chiral resolution or diastereoselective transformations using stoichiometric chiral substrates [8-34]. Unfortunately, both methodologies are cost-intensive and suffer from low synthetic efficiency. Recent years have witnessed a paradigm shift toward highly efficient catalytic asymmetric syntheses to furnish enantioenriched boron stereoisomers. For this reason, the first two traditional approaches are only briefly summarized herein, whereas catalytic asymmetric routes constitute the core focus of this review.

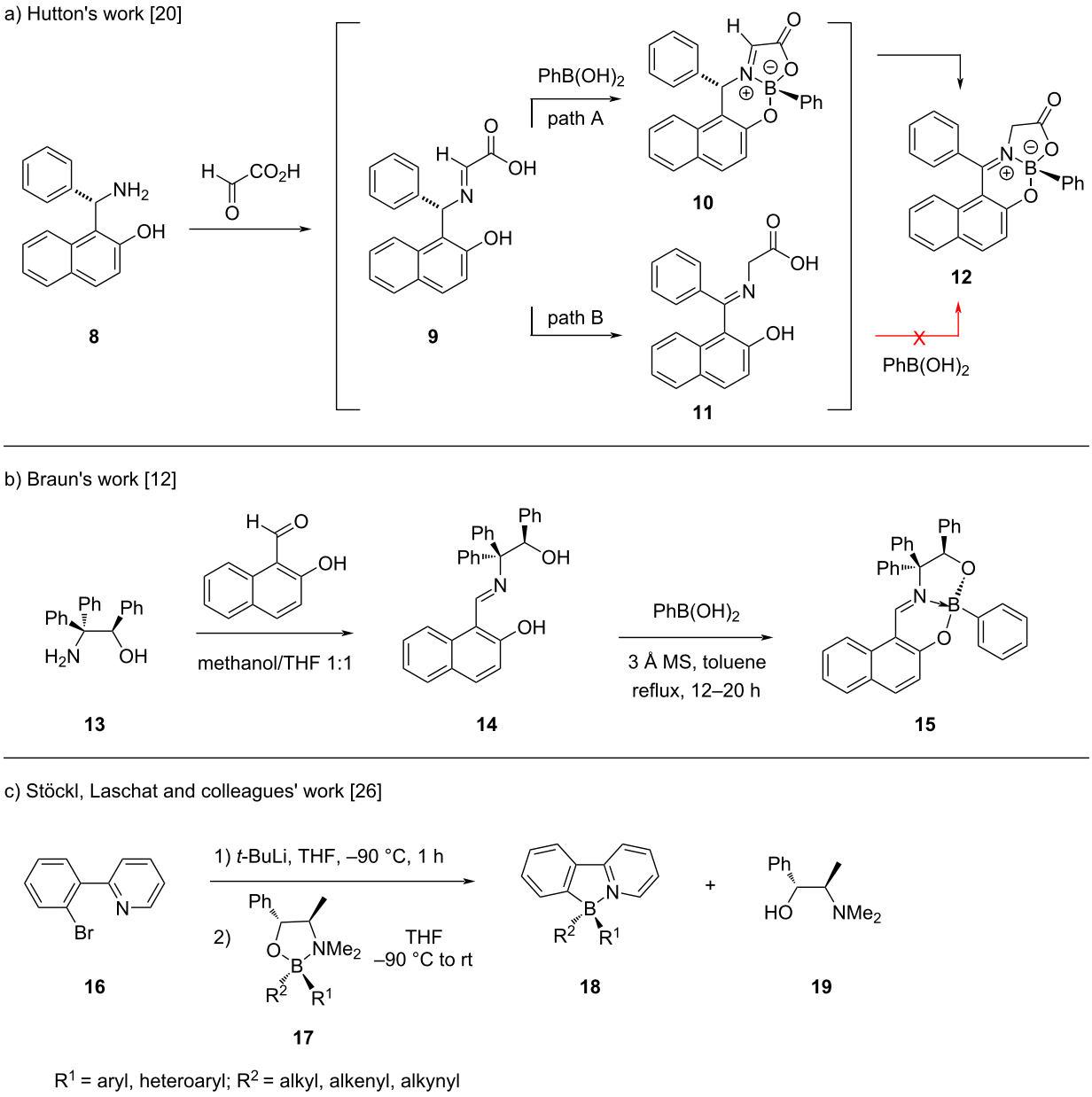
In 1968, Ryschkewitsch and Garrett reported the first successful chiral resolution of tetracoordinate boronium cations [28], which stands as an early milestone toward configurationally stable boron-stereogenic species (Scheme 1a). Their work took BH_2^+ species **1** coordinated with trimethylamine and 4-picoline as the starting platform, furnishing two unsymmetric halo-substituted boronium cations **2** (chloro and bromo derivatives) via a series of high-yield transformations: trimethylamine borane iodination, amine complexation, and borane halogenation. An optically active tris(catecholato)arsenate salt $KAs(C_6H_4O_2)_3$ was utilized as the chiral resolving agent. Stepwise recrystallization of the generated diastereomeric salts enabled effective enantioseparation of the boronium cations, affording pure levorotatory enantiomers alongside partially enriched dextrorotatory fractions. In 1995, Vedejs's group



Scheme 1: Recrystallization or HPLC separation to access chiral boron-centered compounds.

accessed boron-stereogenic compounds **4** and **5** using amino acid-derived chiral amidine carboxylate **3** as the chiral precursor (Scheme 1b) [34]. Subsequent recrystallization delivered the target boron stereoisomers with a single stereoconfiguration. In 2000, Mioskowski's group established a four-step synthetic sequence starting from toluene (**6**) to construct racemic tetracoordinate benzylcyanoborane adducts **7** (Scheme 1c) [8]. Chiral high-performance liquid chromatography (HPLC) was then applied to resolve the enantiomers bearing a stereogenic boron center.

In 2008, Hutton's group established a chirality-transfer strategy employing chiral Betti base **8** as the chiral inducer [20], realizing the first highly enantioselective one-step construction of configurationally stable boronate complexes bearing a single stereogenic boron center (Scheme 2a). The three-component condensation of chiral Betti base **8**, glyoxylic acid and phenylboronic acid proceeded in DMF at 50 °C to deliver complex **12** with boron as the exclusive stereocenter in 97% yield. Two plausible chirality-transfer pathways were proposed. In path A, the amine condenses with glyoxylic acid to generate imine **9**,



Scheme 2: Chiral substrate-induced boron-centered chiral compounds.

while phenylboronic acid reacts with the carboxyl and hydroxy moieties to furnish intermediate **10**. Subsequent imine double-bond isomerization transfers stereochemistry to afford product **12**. By contrast, in path B, imine tautomerization prevents intermediate **11** from establishing a stereogenic center, thus failing to induce boron-centered chirality. That same year, Braun's group disclosed an analogous protocol: chiral (*R*)-amino alcohol **13** was converted to chiral imine **14**, which underwent condensation with phenylboronic acid under reflux to furnish boron-stereogenic species **15** (Scheme 2b) [12]. In 2023, Stöckl, Laschat and colleagues developed a two-step chirality-transfer route toward boron-centered *C*,*N*-chelate complexes (Scheme 2c) [26]. A chiral amino alcohol was first used as a chiral auxiliary to generate the racemic *O*,*N*-heterocyclic boron intermediate **17** through an achiral assembly step. Subsequently, intermediate **17** underwent ligand exchange with the lithiated species generated in situ from 2-(2-bromophenyl)pyridine (**16**). Efficient chirality transfer at boron afforded the target *C*,*N*-chelate complex **18**, together with the recovered amino alcohol **19**.

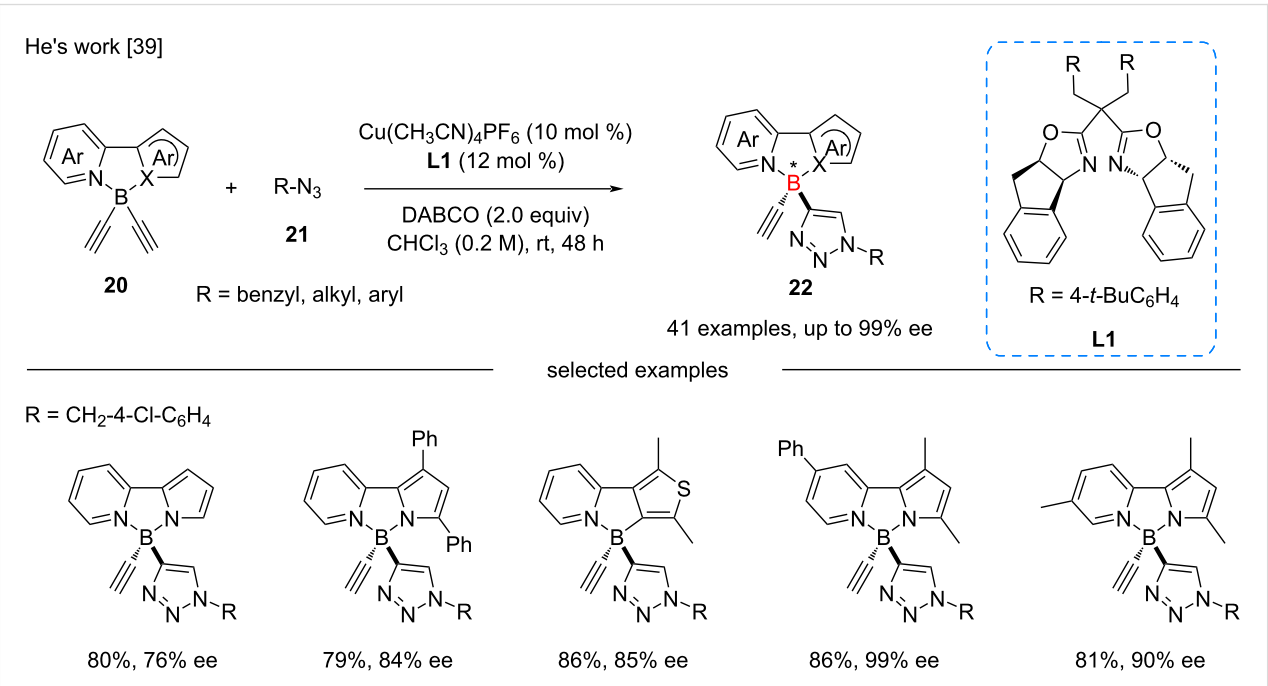
Asymmetric catalysis represents an ideal platform for the streamlined assembly of chiral molecules, yet the catalytic asymmetric construction of stereogenic boron centers has only been achieved within the past few years. This review comprehensively summarizes established asymmetric catalytic routes to boron-stereogenic compounds, categorizing six dominant synthetic tactics: copper catalysis, palladium catalysis, rhodium catalysis, nickel/cobalt catalysis, organocatalysis, and phase-transfer catalysis. We hope this overview will facilitate the exploration of novel synthetic protocols for configurationally stable tetracoordinate boron species and broaden their practical utility in asymmetric catalysis, pharmaceutical development, and functional material fabrication [35-38].

Review

Copper catalysis

In 2021, He's group reported the first catalytic asymmetric route to boron-stereogenic species (Scheme 3) [39]. This work addressed the longstanding challenge of stabilizing stereogenic tetrahedral boron centers, whose lability arises from facile ligand dissociation. Overcoming the drawbacks of traditional separation and chiral-substrate-induced protocols, the group established an innovative asymmetric synthesis relying on a copper(I)-catalyzed azide–alkyne cycloaddition (CuAAC). Boron-bearing substrates **20** served as starting materials, organic azides **21** acted as the cycloaddition partners, and enantiocontrol was realized via synergistic coordination between the copper catalyst and chiral ligand **L1**. This protocol efficiently furnished a library of densely functionalized chiral boron heterocycles **22**, featuring high yields, excellent enantioselectivity, and broad functional-group tolerance across diverse substituents.

Single-crystal X-ray diffraction unambiguously confirmed the absolute configuration at each stereogenic boron center in these

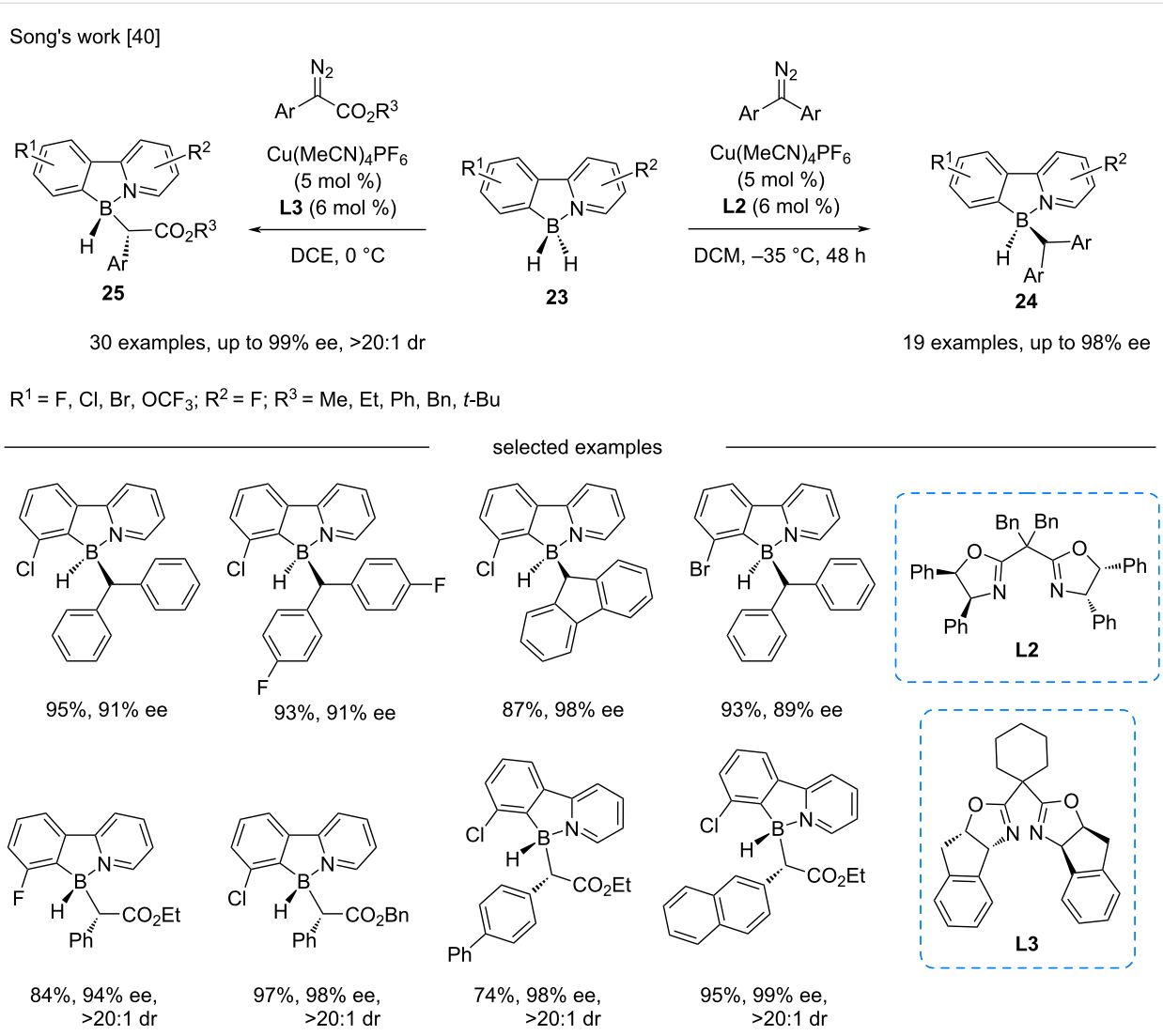


Scheme 3: Catalytic synthesis of boron-stereogenic compounds via asymmetric CuAAC reaction.

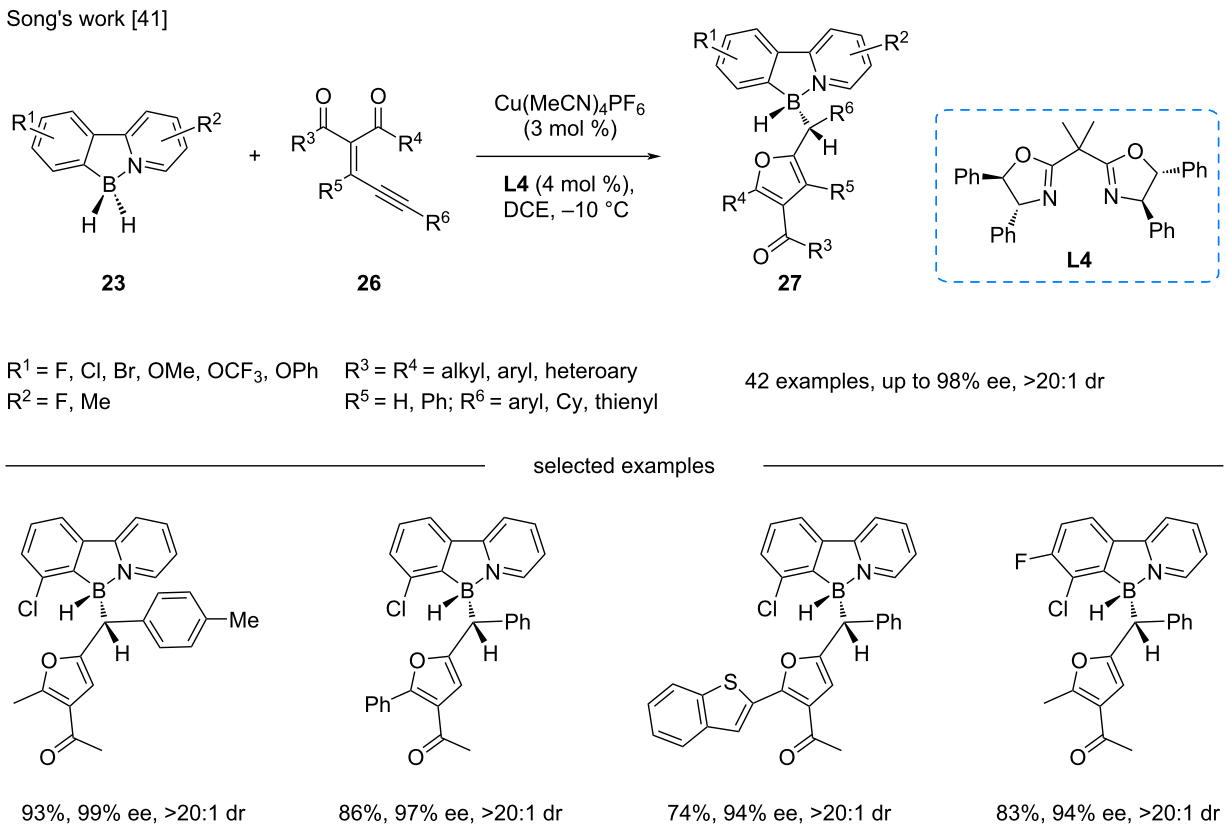
tetracoordinate boron complexes and racemization barrier measurements further verified their configurational stability. Additionally, these π-conjugated boron compounds display prominent chiroptical responses, including distinct circular dichroism (CD) and circularly polarized luminescence (CPL) signals. This pioneering work not only fills a gap in catalytic asymmetric construction of boron-centered chirality but also enriches synthetic methodologies for main-group stereogenic heteroatom compounds.

In 2022, Song's group reported a copper-catalyzed asymmetric desymmetrization via enantioselective B–H carbene insertion (Scheme 4) [40]. This transformation employs 2-arylpyridineborane scaffolds **23** as the starting material and diazo species as carbene precursors. With copper(I) hexafluoroantimonate as the catalyst and chiral bis(oxazoline) ligands **L2** or **L3** in acetonitrile, the reaction furnished boron-stereogenic products **24** and **25** through stereoselective B–H insertion. Conducted under mild conditions, this protocol delivered up to 99% enantiomeric excess (ee) and a diastereomeric ratio (dr) greater than 20:1. Further, the stereogenic boron center retained its configuration throughout subsequent derivatization steps. Combined experimental observations and density functional theory (DFT) computations revealed that substituents at the C7 position of the 2-arylpyridineborane scaffold are critical to attaining such high levels of enantiocontrol in the asymmetric carbene insertion.

In 2023, Song's group achieved another advance in boron-stereogenic synthesis (Scheme 5) [41]. They constructed molecules bearing adjacent boron and carbon stereocenters through a copper-catalyzed asymmetric B–H carbene insertion. This protocol employed alkynone **26** as a furanyl carbene precursor



Scheme 4: Catalytic synthesis of boron-stereogenic compounds via desymmetric B–H bond insertion reaction.



Scheme 5: Copper-catalyzed synthesis of boron–carbon dual stereogenic compounds via a desymmetrization B–H bond-insertion reaction.

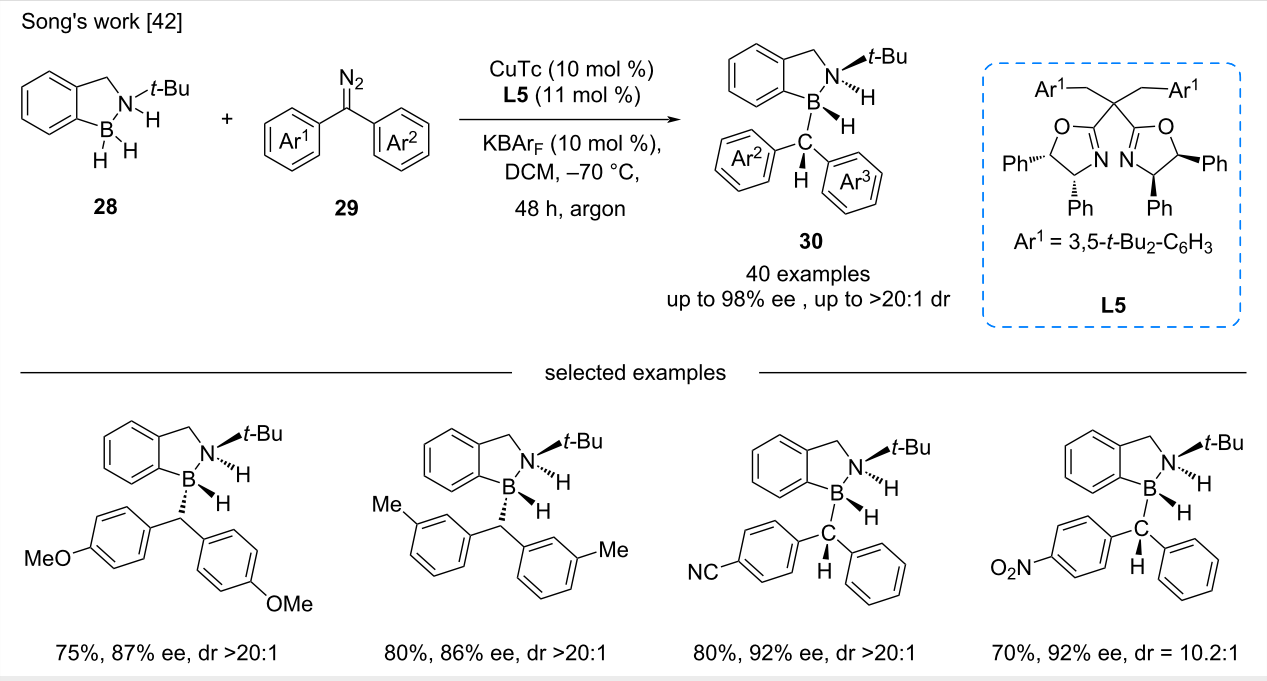
and 2-arylpyridine-boranes **23** as the starting substrates. With copper(I) hexafluorophosphate paired with chiral bis(oxazoline) (BOX) ligand **L4**, the in situ formed copper furanyl carbene underwent enantioselective insertion into the B–H bond, rapidly delivering densely functionalized adducts **27** featuring contiguous boron–carbon stereogenic centers.

In 2025, Song's group established an innovative catalytic asymmetric protocol to assemble continuous heteroatomic stereogenic centers via copper-catalyzed B–H insertion reaction (Scheme 6) [42]. This transformation employed racemic cyclic amine boranes **28** and diaryldiazomethanes **29** as starting materials, forging vicinal nitrogen–boron stereocenters as well as sequential nitrogen–boron–carbon contiguous stereogenic frameworks **30**. The core of this method lies in the effective configuration locking of the nitrogen stereocenter through boron–nitrogen coordination, together with a concurrent kinetic-resolution pathway for racemic amine borane substrates. This synthetic route bears remarkable merits: broad substrate compatibility, excellent diastereo- and enantioselectivity, and the recovered enantioenriched amine borane can act as chiral transfer-hydrogenation reagents. DFT calculations further unveiled that substrate π–π stacking and ligand-induced steric distortion collectively account for the observed stereoselectivity.

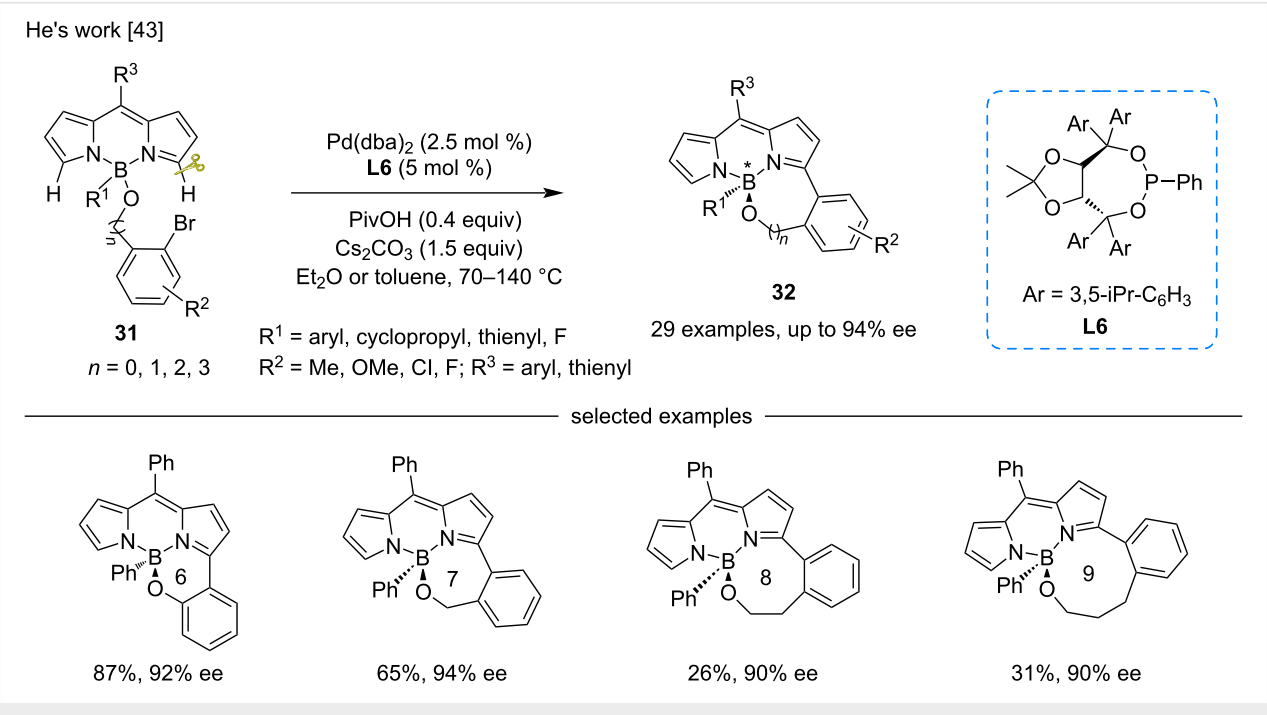
Palladium catalysis

In 2023, He's group realized the first catalytic asymmetric route to boron-stereogenic BODIPY (boron-dipyrromethene) derivatives (Scheme 7) [43]. Their synthetic design relied on a palladium-catalyzed desymmetrization via an intramolecular C–H arylation. The delocalized BODIPY scaffold **31** was chosen as the starting material, and stereocontrol at the boron center was finely tuned by matching the Pd catalyst with tailored chiral ligand **L6**. This protocol readily assembled six-membered boron-containing stereogenic rings and could be extended to access seven- to nine-membered analogues **32** without compromising enantioselectivity.

This work addressed a longstanding synthetic bottleneck: previously, boron-stereogenic BODIPYs could only be isolated via chiral resolution. The resulting complexes displayed outstanding chiroptical performances and hold great promise for chiral recognition. More broadly, this methodology established a facile route to boron-stereogenic BODIPYs and delivered guiding principles for synthesizing other heteroatom-stereo-



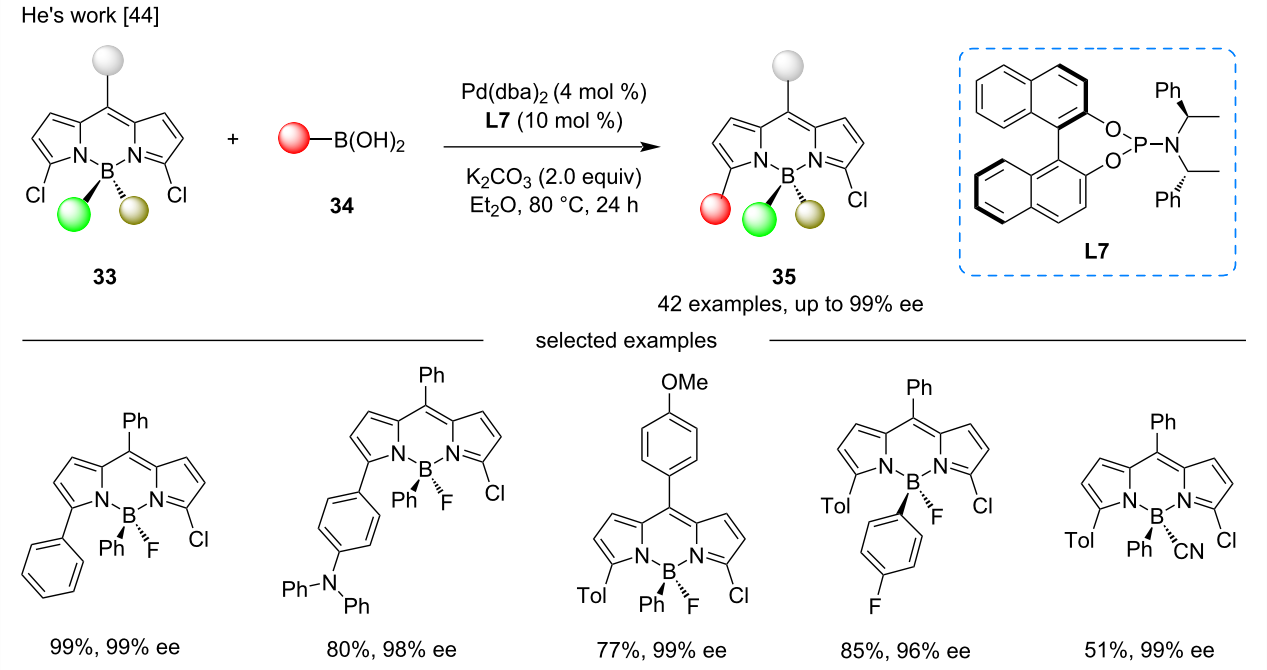
Scheme 6: Catalytic synthesis of nitrogen–boron–carbon continuous stereocenter compounds via asymmetric B–H bond insertion reaction. CuTc = copper(I) thiopene-2-carboxylate hydrate, $KBAr_F$ = potassium tetrakis(perfluorophenyl)borate.



Scheme 7: Catalytic synthesis of boron-stereogenic BODIPYs via desymmetric intramolecular C–H arylation reaction.

genic molecules, and broadened both the research scope and application prospects of boron stereochemistry.

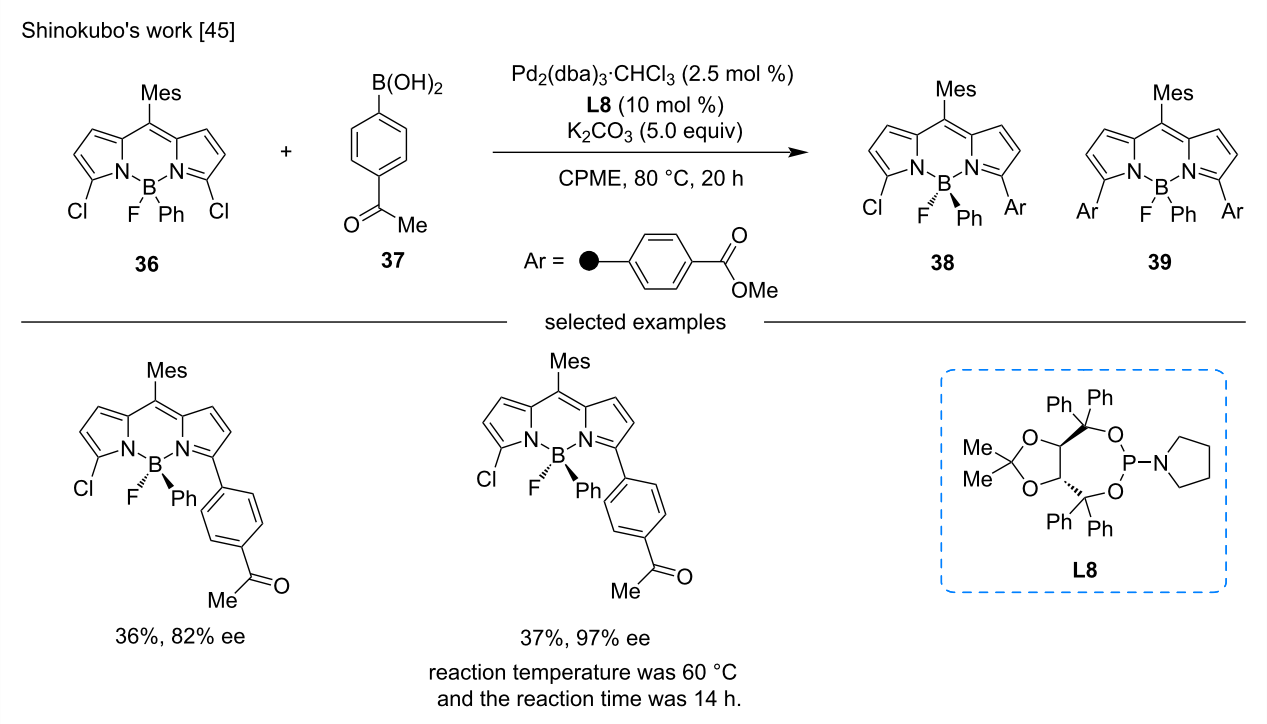
In 2025, He's group disclosed a novel desymmetrization protocol based on a palladium-catalyzed Suzuki–Miyaura cross-coupling (Scheme 8) [44]. The reaction utilized prochiral 3,5-dichlorinated boron-dipyrromethene (BODIPY) scaffold **33** and various boron coupling partners **34** (arylboronic acids, vinylboronate derivatives) as starting materials, rapidly assembling polysubstituted boron-stereogenic BODIPY derivatives **35**. The



Scheme 8: Synthesis of boron-stereogenic compounds via a palladium-catalyzed desymmetrization Suzuki cross-coupling reaction.

core of this method lies in the precise discrimination of the two α-C–Cl bonds on the prochiral BODIPY backbone. This synthetic route features remarkable merits: high modularity, outstanding stereoselectivity, and broad functional-group tolerance.

In 2025, Shinokubo's group reported an enantioselective desymmetrization strategy via a palladium-catalyzed intermolecular Suzuki–Miyaura coupling (Scheme 9) [45]. The reaction of BODIPY substrate **36** with arylboronic acid **37** afforded



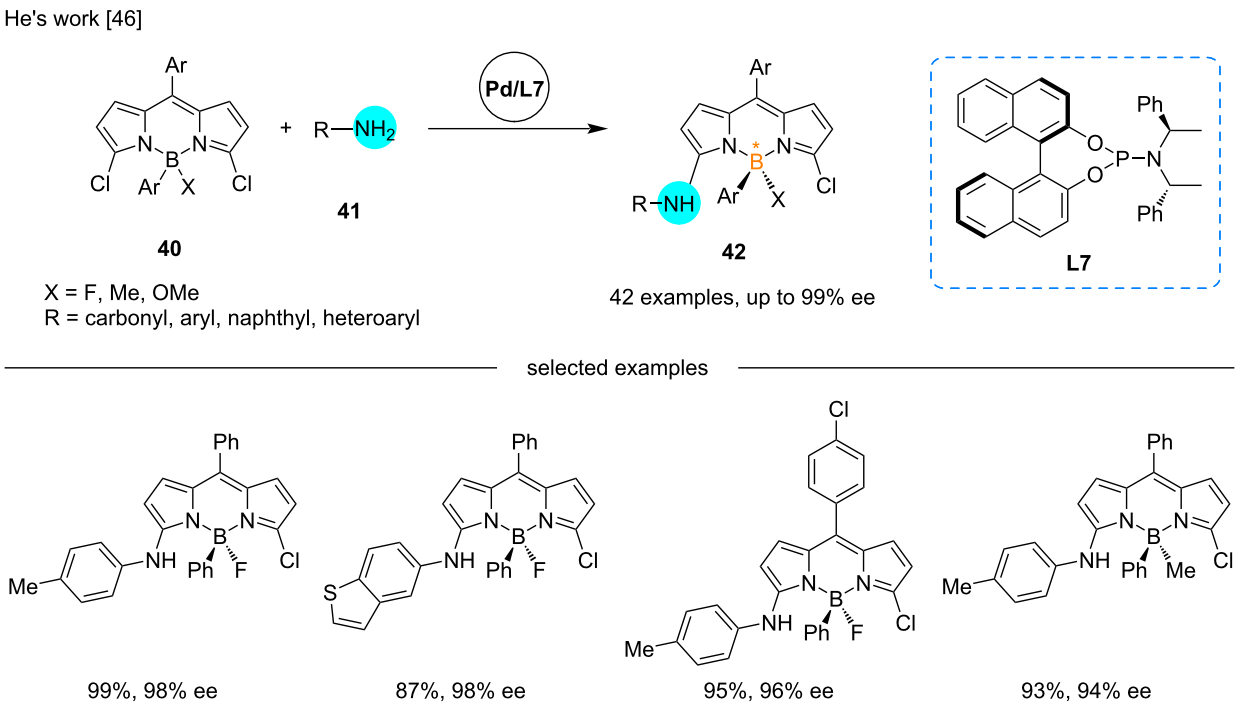
Scheme 9: Catalytic construction of a stereogenic boron center on BODIPY derivative **36** via enantioselective Suzuki–Miyaura coupling.

the boron-stereogenic monoarylated BODIPY **38**. Importantly, the monoarylated product can undergo a second arylation to form diarylated, achiral BODIPY **39**. Mechanistic studies revealed that this second coupling preferentially consumes the minor enantiomer of **38**, thereby enhancing the enantiomeric excess of the remaining monoarylated product through kinetic resolution. This protocol afforded boron-stereogenic BODIPYs with enantioselectivities of up to 97% ee. Furthermore, the introduction of aryl substituents modulated the photophysical properties of BODIPY, resulting in bathochromic shifts in both the absorption and emission spectra.

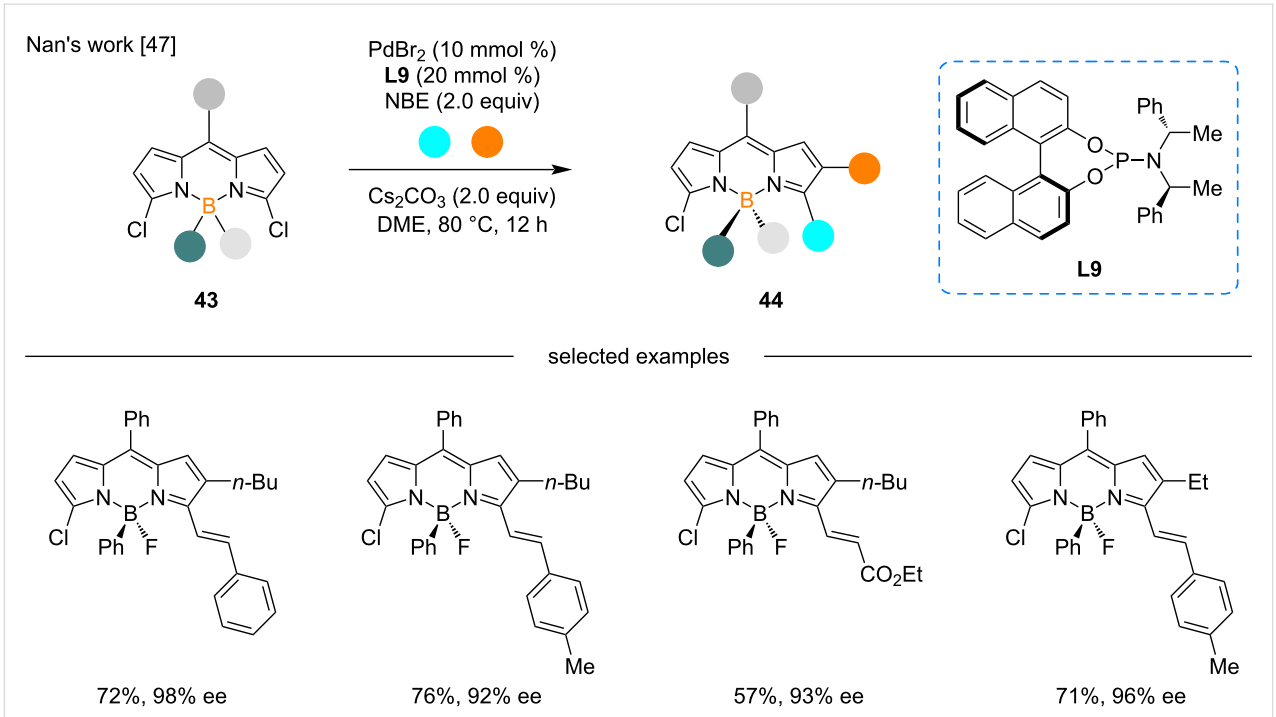
In 2025, He's group developed a palladium-catalyzed asymmetric C–N cross-coupling approach (Scheme 10) [46], with prochiral 3,5-dihalogenated BODIPY scaffolds **40** and various amines **41** as the starting substrates. With the catalyst combination and reaction parameters appropriately tuned, asymmetric desymmetrization enabled the efficient assembly of boron-stereogenic 3-amino-BODIPY derivatives **42**. This synthetic protocol possesses prominent merits: broad substrate scope, excellent functional-group tolerance, and high stereocontrol. A wide range of nucleophiles is suitable, including aromatic amines, heteroaromatic amines, and amides bearing electron-donating (methyl, methoxy) or electron-withdrawing substituents (ester, trifluoromethyl, cyano). Furthermore, the reaction tolerates diverse boron-attached substituents such as naphthyl, thionyl, and methyl. A library of structurally diverse boron-stereogenic 3-amino-BODIPYs was therefore furnished with ee values reaching 99%.

In 2026, Nan's group established a cooperative palladium/norbornene asymmetric Catellani desymmetrization protocol (Scheme 11) [47]. Starting from dichlorinated prochiral BODIPY scaffolds **43**, the one-step difunctionalization with alkenes and alkyl iodides enabled the rapid assembly of polysubstituted boron-stereogenic BODIPY derivatives **44**. This catalytic system combines palladium(II) bromide with the BINOL-based chiral phosphoramidite ligand **L9** and norbornene, which efficiently inhibited undesired Heck side reactions and stereochemical racemization at the stereogenic boron center.

The reaction displayed a remarkably broad substrate generality and delivered 87 distinct functionalized adducts, most of which afforded ee values up to 99%. Various alkenes, alkyl iodides, and intricate natural-product- or drug-derived skeletons were well tolerated. The isolated boron-stereogenic products feature robust configurational stability and can undergo versatile post-modifications such as cross-coupling, nucleophilic substitution, kinetic resolution, and iterative dual Catellani transformations to access dimeric fluorescent dyes. Upon π-conjugation elongation, these fluorophores displayed pronounced spectral red



Scheme 10: Synthesis of boron-centered compounds via palladium-catalyzed asymmetric carbon-nitrogen cross-coupling reaction.

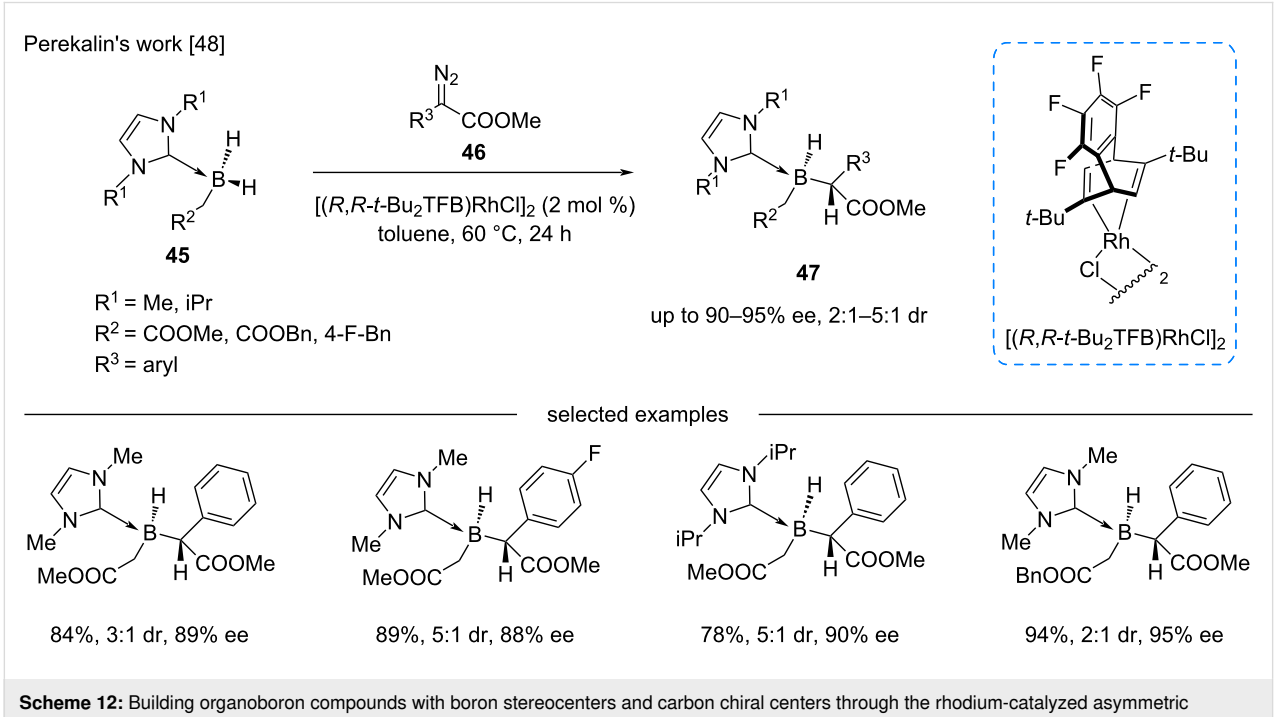


Scheme 11: Synthesis of boron-stereogenic compounds via palladium/norbornene synergistic asymmetric Catellani reaction. NBE = norbornene.

shifts and distinct chiroptical signatures. Cellular assays further verified their low cytotoxicity and favorable cellular uptake, rendering them promising candidates for near-infrared bioimaging and chiral optoelectronic devices.

Rhodium catalysis

In 2024, Perekalin's group reported a rhodium(I)-catalyzed asymmetric carbene insertion enabled by chiral diene ligands (Scheme 12) [48]. This transformation inserts aryldiazoacetates



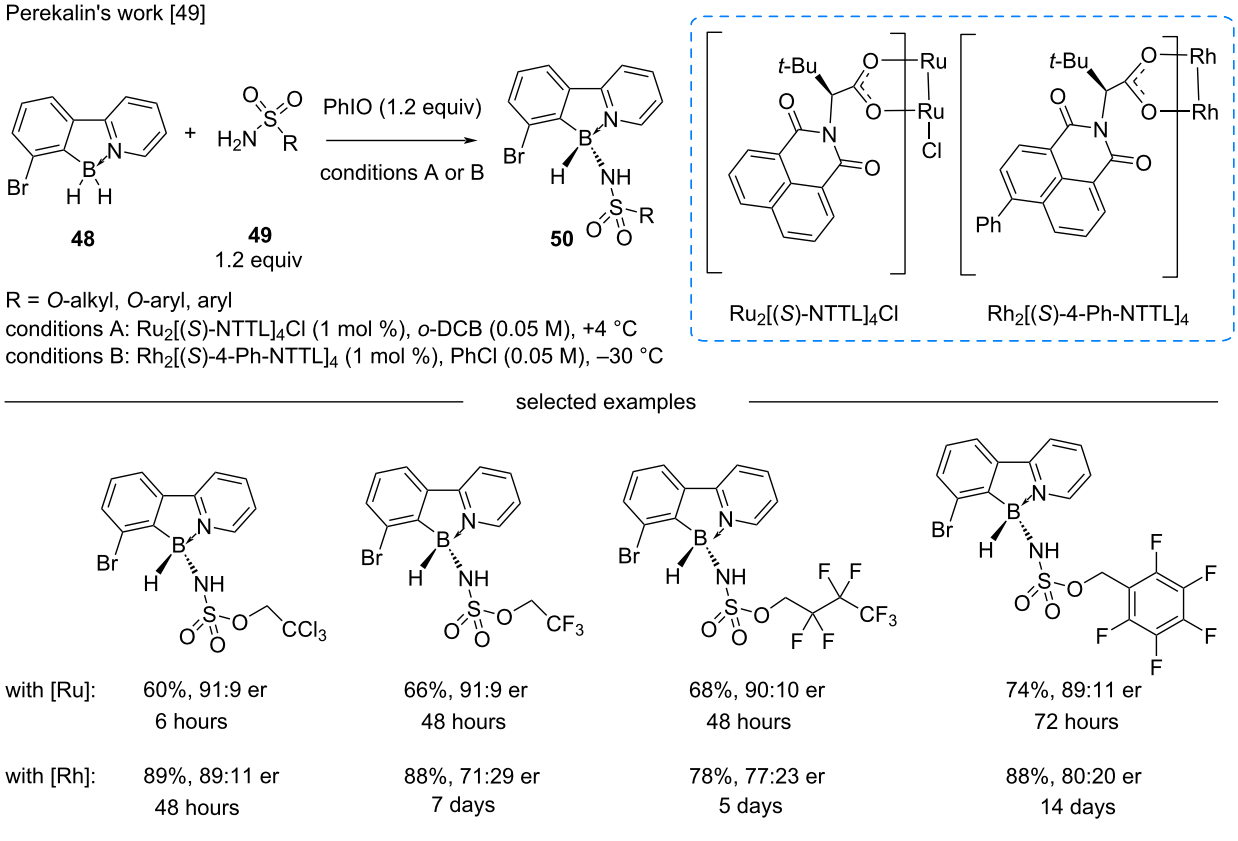
Scheme 12: Building organoboron compounds with boron stereocenters and carbon chiral centers through the rhodium-catalyzed asymmetric carbene insertion into B–H bonds.

46 into the B–H bond of N-heterocyclic carbene (NHC) borane **45**, furnishing, for the first time, organoboron adducts **47** that bear both carbon and boron stereocenters through a single catalytic step. The optimal catalyst was a rhodium dimer coordinated with a chiral *t*-Bu$_2$-TFB (tetrafluorobenzobarrelene) ligand. Under the established conditions, the target products were obtained in 75–90% yields with diastereomeric ratios (dr) ranging from 2:1 to 5:1, and the major diastereomers reached ee values of 90–95%. The protocol features straightforward operation, and most isolated products displayed robust stability toward air and moisture.

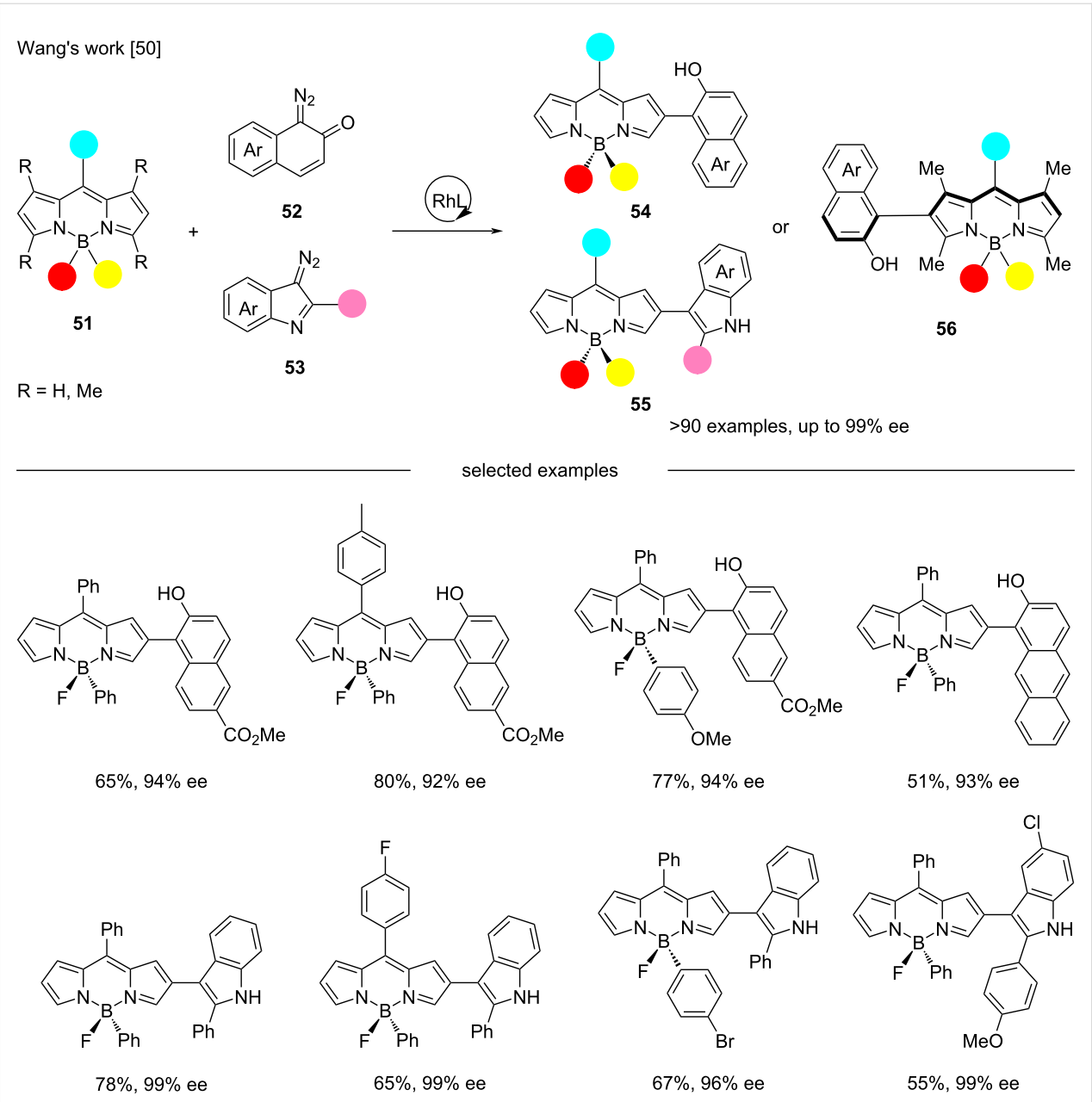
In 2025, Perekalin's group further established a dirhodium/diruthenium-catalyzed nitrene insertion into B–H bonds (Scheme 13) [49]. This catalytic manifold enabled the one-step assembly of organoboron adducts **50** bearing boron-stereogenic centers and covalent B–N linkages for the first time, and it still remains the sole asymmetric route capable of constructing stereogenic B–N bonds. The protocol relies on dinuclear rhodium and ruthenium carboxylate complexes modified with chiral NTTL ligands, with prochiral phenylpyridine borane **48** serving as the starting substrate. Stereochemical induction was tuned by low reaction temperature and tailored solvent media. Amino sulfonamides **49** bearing electron-poor oxymethylene substituents deliver the best performance, affording a maximum enantiomeric ratio (er) of 91:9.

In 2025, Wang's group disclosed a rhodium(II)-catalyzed enantioselective C–H (hetero)arylation protocol (Scheme 14) [50]. The transformation employed prochiral BODIPY scaffold **51**, diazonaphthoquinones (DNQs) **52** and diazoindoles (DINs) **53** as starting feedstocks. Via remote desymmetrization and sterically enforced restriction of axial rotation, the reaction rapidly furnished boron-stereogenic BODIPYs **54**, **55**, and axially chiral BODIPY analogues **56** in a single operation. This constitutes the first catalytic platform enabling the one-pot assembly of both boron-stereogenic and axially chiral BODIPYs, with prominent merits including site-selective reactivity, broad substrate generality, and outstanding stereocontrol. The route surmounts the drawbacks of conventional methods, which lack straightforward access to β-functionalized BODIPYs bearing diverse stereogenic motifs, and opens up new avenues for fabricating functional chiral fluorophores.

In 2025, Fang's group established a rhodium-catalyzed asymmetric cyclization protocol (Scheme 15) [51]. Relying on a



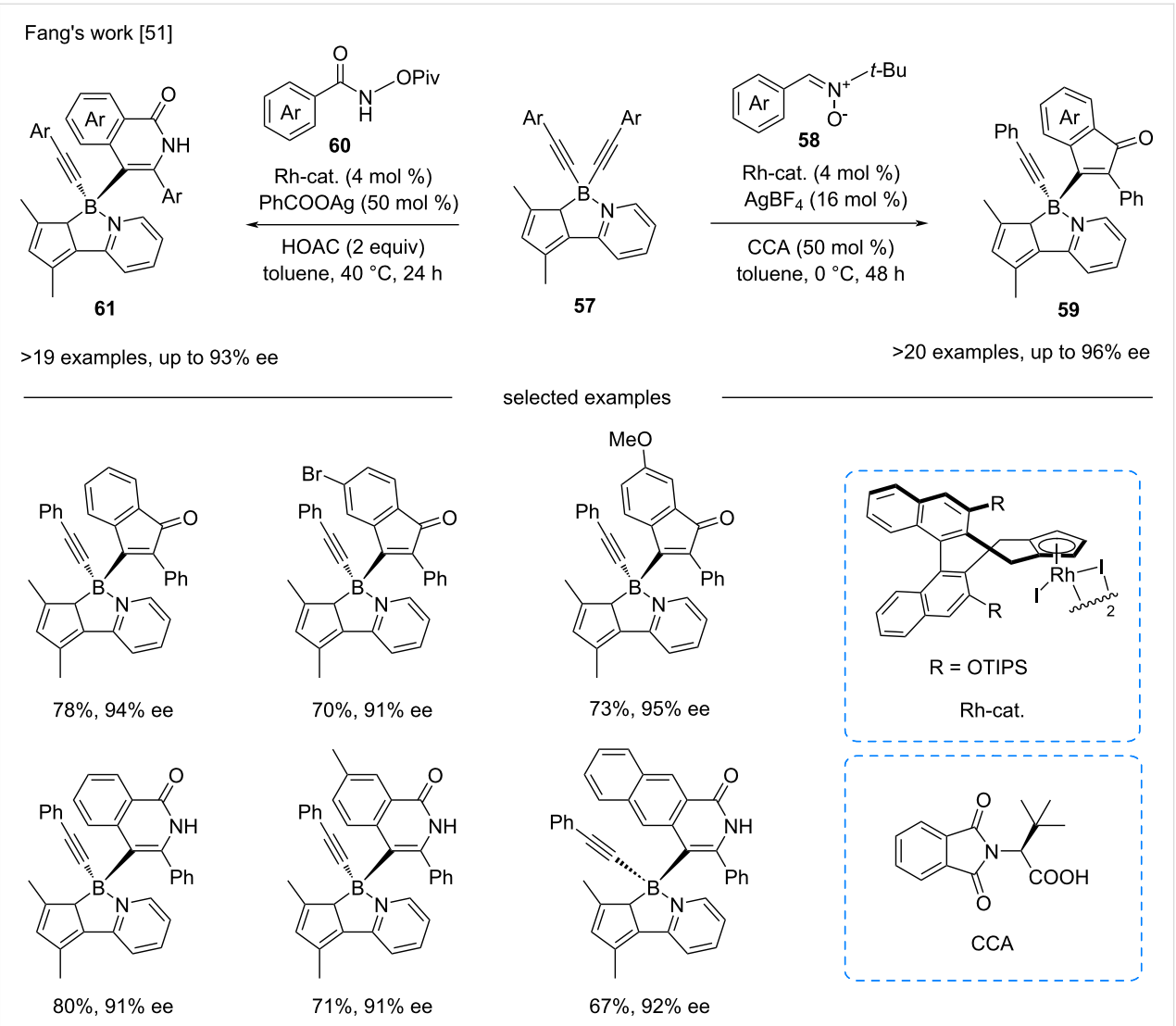
Scheme 13: Synthesis of chiral boron compounds through desymmetrization B–H insertion reactions catalyzed by dirhodium/diruthenium complexes.



Scheme 14: Divalent rhodium-catalyzed enantioselective C–H (hetero)arylation reaction for synthesizing boron-chiral BODIPYs and axial-chiral BODIPYs.

rhodium(III)-mediated aromatic C–H activation, this approach realized the desymmetrization of two arene substrates **58** and **60** via a [4 + 2] or [3 + 2] cycloaddition with tetracoordinate bis(alkynyl)boron reagent **57**. The reaction delivered five- and six-membered boron-containing heterocycles **59** and **61** in a single efficient step, each bearing a stereogenic boron center as the exclusive source of chirality. The transformation tolerated aryl, heteroaryl, and pharmaceutical-derived skeletons, and was amenable to gram-scale preparation as well as diverse post-functionalization reactions. Single-crystal X-ray diffraction unambiguously assigned the absolute configuration at the boron atom. Racemization kinetic measurements revealed racemization barriers ranging from 28.5 to 31.7 kcal/mol, demonstrating that the tetrahedral geometry around boron dominates the configurational stability of these heterocyclic products.

In 2025, Xu's group advanced boron-stereogenic syntheses with two distinct catalytic platforms for asymmetric desymmetrizing B–H carbene insertion: Rh(I)/chiral diene and Cu(I)/chiral bis(oxazoline) (BOX) systems, which enabled the stereodiver-



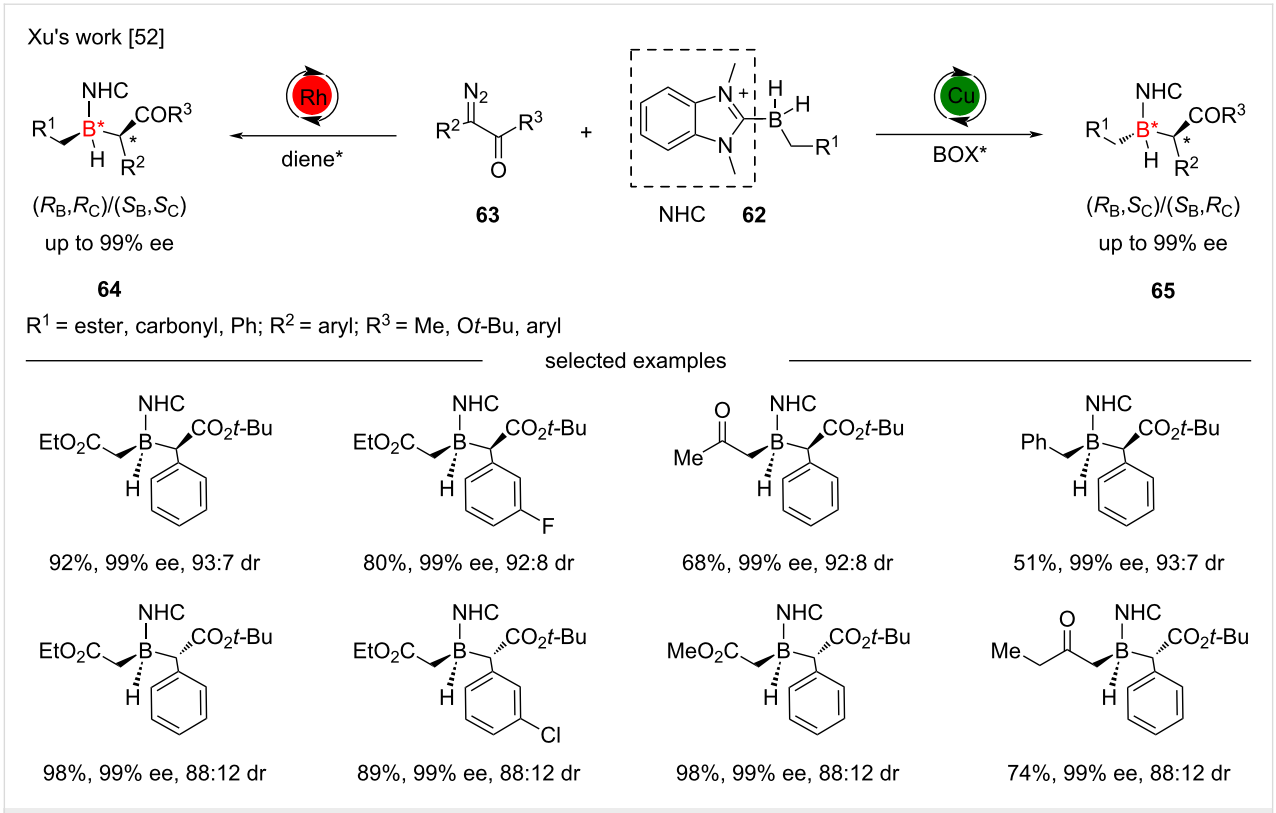
Scheme 15: Rhodium(III)-catalyzed asymmetric cyclization reaction for synthesizing boron-stereogenic compounds.

gent assembly of contiguous carbon and boron stereogenic centers (Scheme 16) [52]. This protocol uses chiral N-heterocyclic carbene (NHC) borane **62** as the boron source instead of simple dihydroboranes, with aryldiazo esters and diazo ketones **63** serving as carbene precursors. Under Rh–chiral diene catalysis or $Cu(MeCN)_4PF_6$ paired with chiral BOX ligands, a metal–carbene-mediated enantioselective insertion into the B–H bond furnished the densely functionalized organoboron adducts **64**, **65** bearing configurationally stable stereogenic boron and carbon centers.

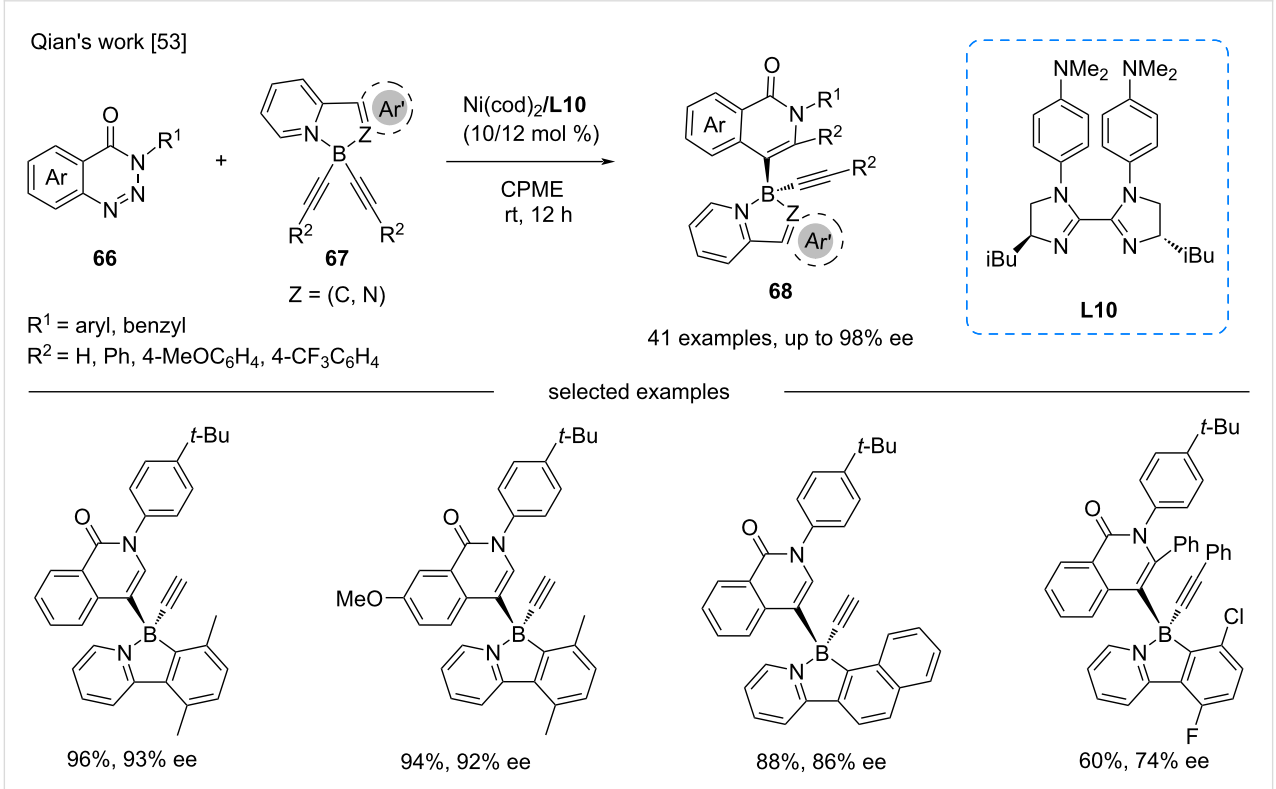
Notably, the two catalytic manifolds deliver reversed diastereocontrol. Matching each catalyst with enantiomeric chiral ligands grants selective access to all four possible stereoisomers. The isolated products featured boron centers with up to 91.1% tetrahedral character and robust stereochemical thermal stability. This transformation demonstrated broad substrate generality, delivering the products in yields as high as 99%, dr values up to 93:7, and nearly uniform 99% ee for most substrates.

Nickel/cobalt catalysis

In 2025, Qian's group reported a Ni(0)-catalyzed asymmetric denitrogenative cyclization to access boron-stereogenic heterocycles (Scheme 17) [53]. This transformation couples 1,2,3-benzotriazinones **66** with diynylboron reagents **67**, using chiral bis(imidazoline) (BiIM) ligand **L10** to coordinate the nickel center. $Ni(cod)_2$ served as the precatalyst, and the desymmetrization proceeded efficiently at room temperature under neat, solvent-free conditions to deliver a library of boron-stereogenic N–B heterocycles **68** with yields up to 96% and ee values reaching 98%. The protocol featured broad substrate generality and was readily scalable to gram quantities. The terminal alkyne



Scheme 16: Synthesis of boron-stereogenic compounds via Rh(I)/Cu(I)-catalyzed enantioselective B–H insertion.



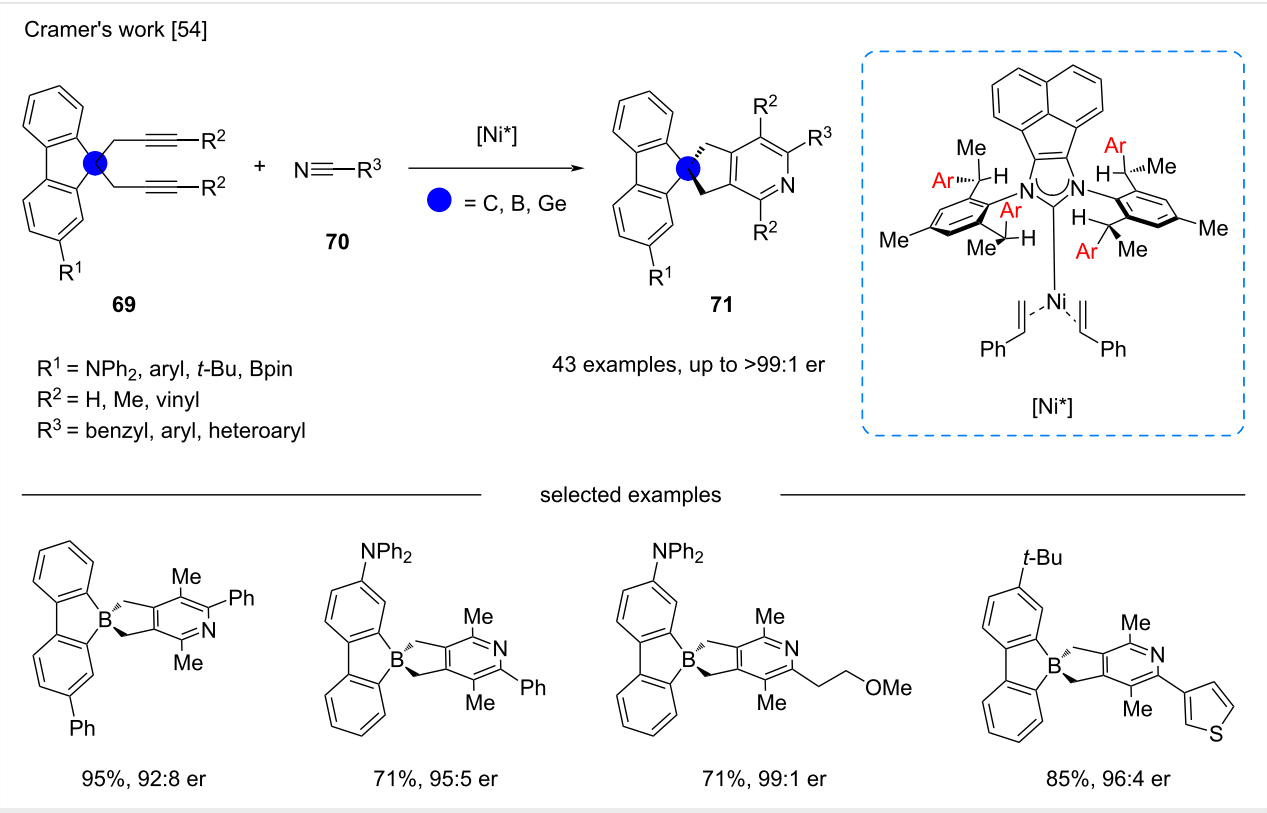
Scheme 17: Synthesizing boron chiral compounds through nickel-catalyzed cyclization and desymmetrization.

moieties embedded within the products were amenable to diverse post-functionalizations including Sonogashira cross-coupling, alkyne hydrogenation, and [3 + 2] cycloaddition reactions, with the stereoconfiguration at each boron-stereogenic center fully retained throughout all transformations.

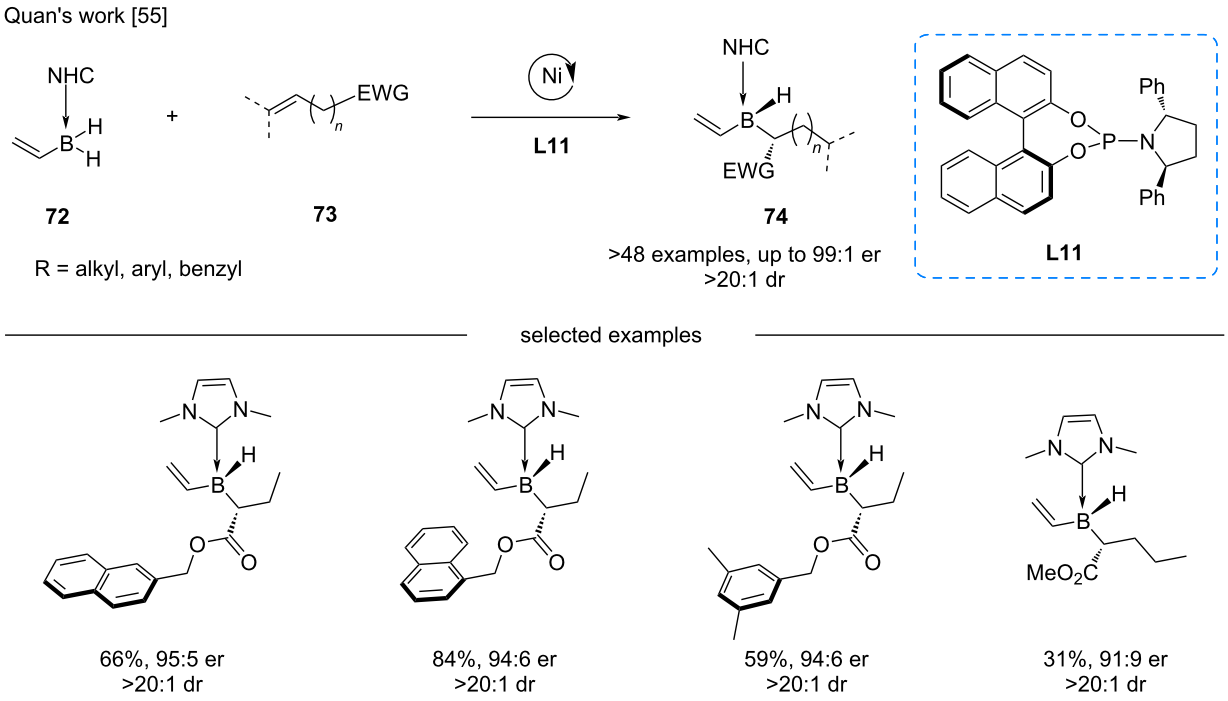
In 2025, Cramer's group disclosed a unified enantioselective [2 + 2 + 2] cycloaddition platform mediated by chiral NHC-Ni(0) complexes (Scheme 18) [54]. This single catalytic manifold enabled the concurrent construction of spirocyclic frameworks bearing carbon-, boron-, and germanium-stereogenic centers. The transformation employed diyne-tethered carbon, boron, and germanium precursors **69** alongside diverse nitrile substrates **70**. Through remote desymmetrization, long-range stereochemical induction was realized, facilitating the streamlined assembly of pyridine-fused chiral spirocycles **71** under mild ambient conditions. Several target adducts delivered quantitative yields and enantiomeric ratios exceeding 99:1. This protocol exhibits outstanding substrate generality, tolerating aromatic, aliphatic and heteroaromatic nitriles as well as heavily functionalized diyne precursors built around carbon, boron, or germanium backbones.

In 2026, Quan's group established a Ni(0)/sterically encumbered chiral phosphoramidite catalytic system, realizing for the first time an asymmetric hydroboration to forge stereogenic boron centers (Scheme 19) [55]. This work overcame the long-standing constraint that conventional alkene asymmetric hydroboration exclusively generates carbon-stereogenic centers and fails to deliver sp^3-hybridized stereogenic boron moieties. The transformation enabled the one-step generation of contiguous carbon- and boron-stereogenic centers, furnishing acyclic tetracoordinate organoboron derivatives **74** bearing two stereogenic elements. The NHC-coordinated vinyl-substituted prochiral tetracoordinate boron species **72** served as the key substrate, with $Ni(cod)_2$ as the precatalyst and the rigid bulky chiral phosphoramidite **L11** as the optimal ligand. Cesium carbonate-mediated isomerization of alkenes **73** broadened the accessible substrate portfolio, and conducting the reaction in *n*-hexane at low temperature (5 °C) markedly enhanced enantioselectivity. Under optimized conditions, the diastereoselectivity typically exceeded 20:1 dr, the maximum enantiomeric ratio reached 99:1 er, and yields were up to 85%.

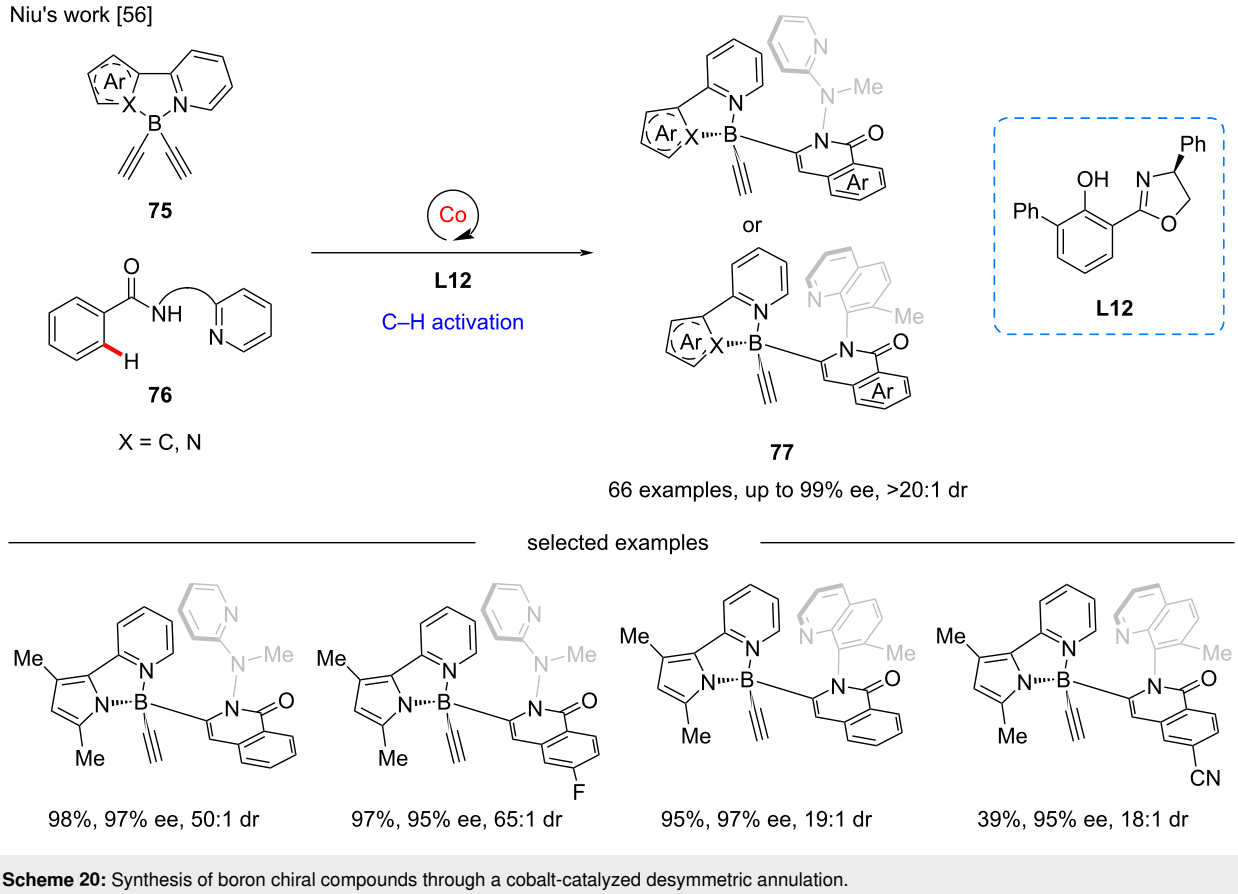
In 2026, Niu's group constructed an earth-abundant cobalt/chiral salicyloxazoline (Salox) catalytic system employing ligand **L12** (Scheme 20) [56]. An asymmetric C–H-activation/desymmetrization cyclization between arylamides **76** and prochiral diynylboron substrates **75** enabled the one-step assembly of tetracoordinate boron-containing heterocycles **77**



Scheme 18: Synthesis of boron chiral compounds through chiral NHC–Ni(0) complexes-catalyzed cyclization and desymmetrization.



Scheme 19: Synthesizing boron chiral compounds through nickel-catalyzed boron-stereogenic hydroboration.

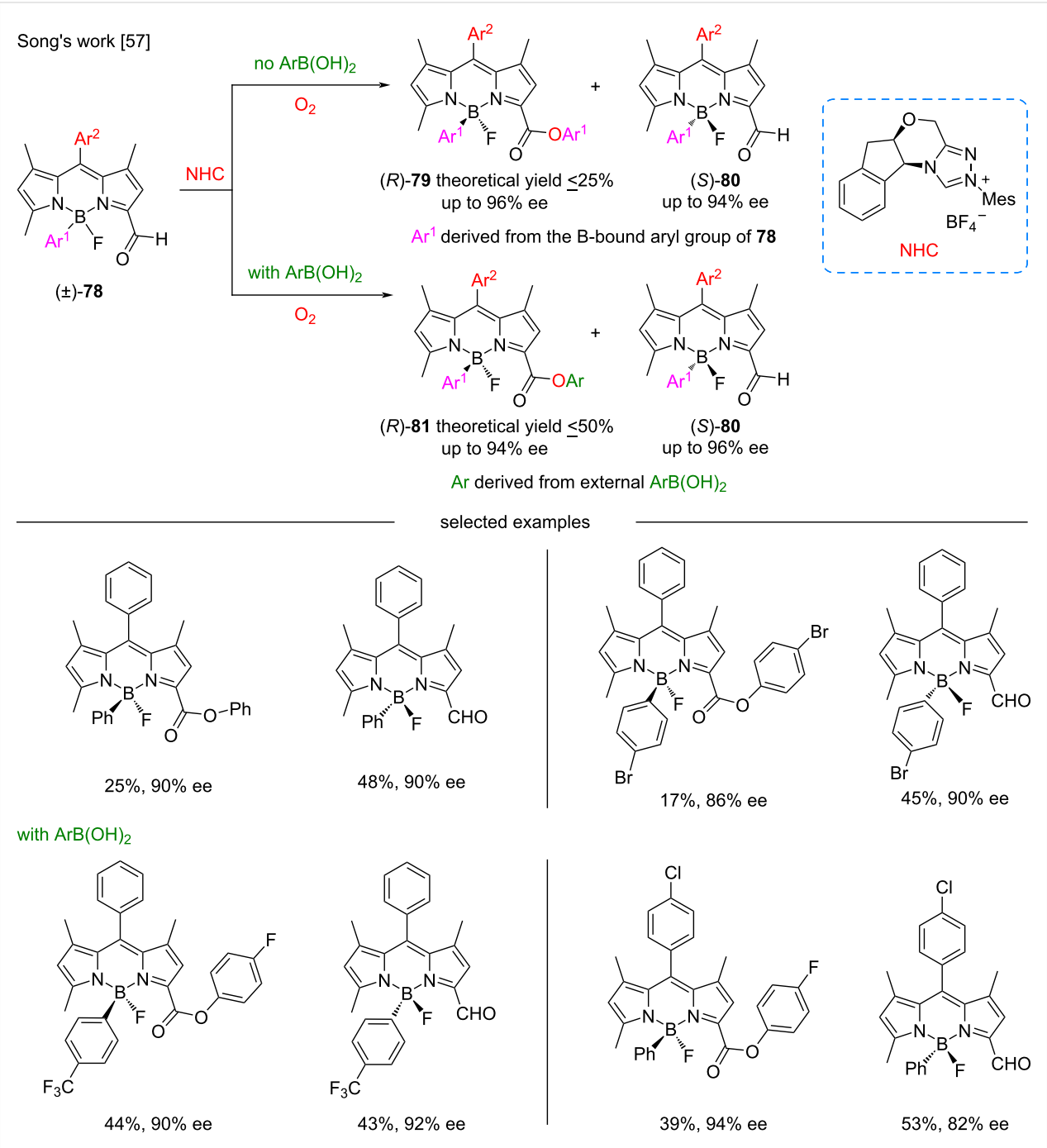


Scheme 20: Synthesis of boron chiral compounds through a cobalt-catalyzed desymmetric annulation.

that simultaneously bear a stereogenic boron center as well as N–N and C–N axial chirality. This represented the first cobalt-catalyzed asymmetric C–H activation strategy for the fabrication of boron-stereogenic compounds.

Organocatalysis

In 2025, Song's group developed an N-heterocyclic carbene (NHC)-catalyzed kinetic resolution strategy using racemic formyl compounds **78** as substrates (Scheme 21) [57]. This oxidative esterification protocol enabled the efficient synthesis of boron-stereogenic formyl compounds **80** and aryl carboxylates **79** and **81**, marking the first implementation of NHC catalysis for constructing boron-stereogenic centers. Under mild oxidative conditions, the NHC catalyst selectively promoted the esterification of one substrate enantiomer to afford carboxylate-functionalized compounds, while the residual enantiomer



Scheme 21: N-Heterocyclic carbene-catalyzed kinetic resolution of racemic formyl compounds through oxidative esterification.

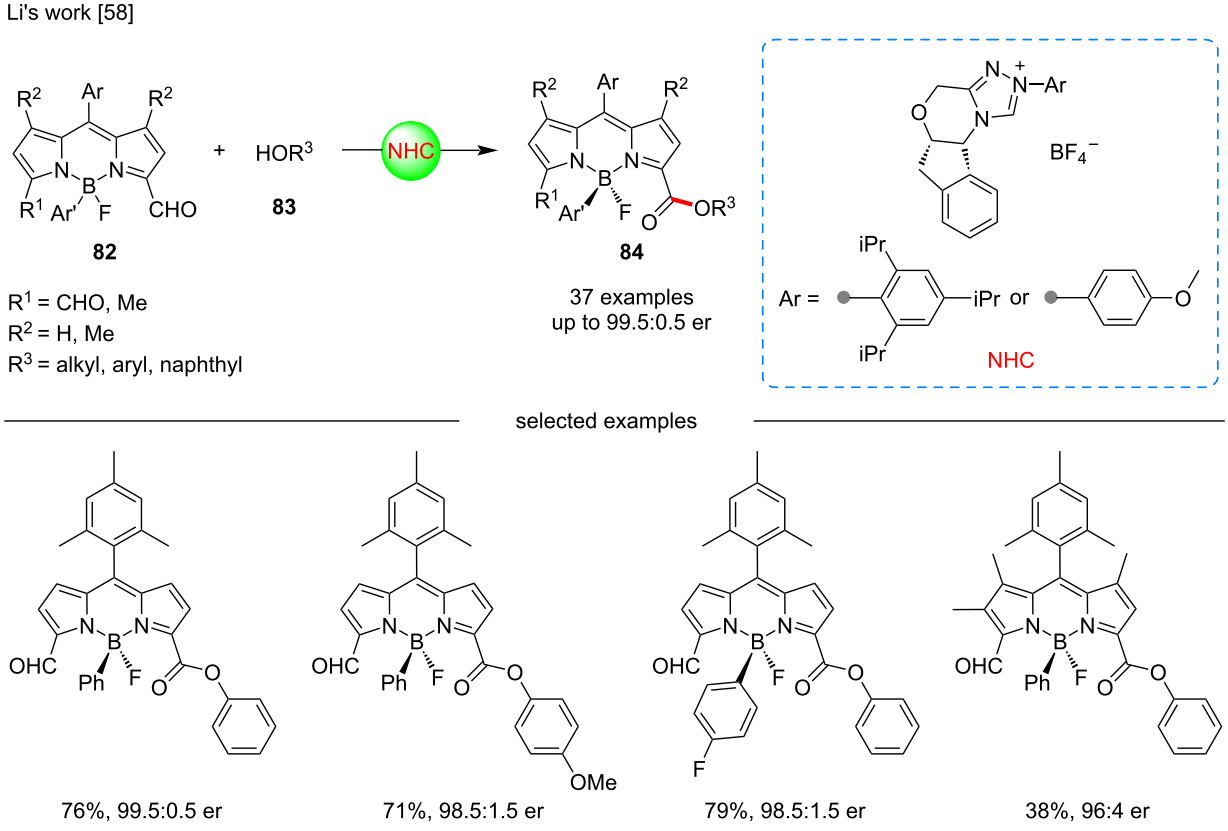
retained with high enantiopurity, thereby realizing effective kinetic resolution. The introduction of arylboronic acids as external nucleophiles further improved the reaction efficiency and stereocontrol, furnishing the target products with ee values up to 96%.

In 2025, Li's group further exploited the N-heterocyclic carbene (NHC)-catalyzed enantioselective esterification (Scheme 22) [58]. Using α,α-diformyl-BODIPYs **82** and diverse phenol and alcohol derivatives **83** as starting materials, the team achieved asymmetric desymmetrization to access boron-stereogenic formyl-BODIPYs **84** in the presence of 3,3′,5,5′-tetra-*tert*-butyl diphenoquinone (DQ), cesium carbonate, and pyridinium *p*-toluenesulfonate (PPTS). This protocol featured excellent stereocontrol and broad functional-group tolerance. It accommodates phenols and alcohols bearing electron-donating or electron-withdrawing substituents, as well as natural-product-derived skeletons, allowing facile access to a diverse library of boron-stereogenic formyl-BODIPY derivatives.

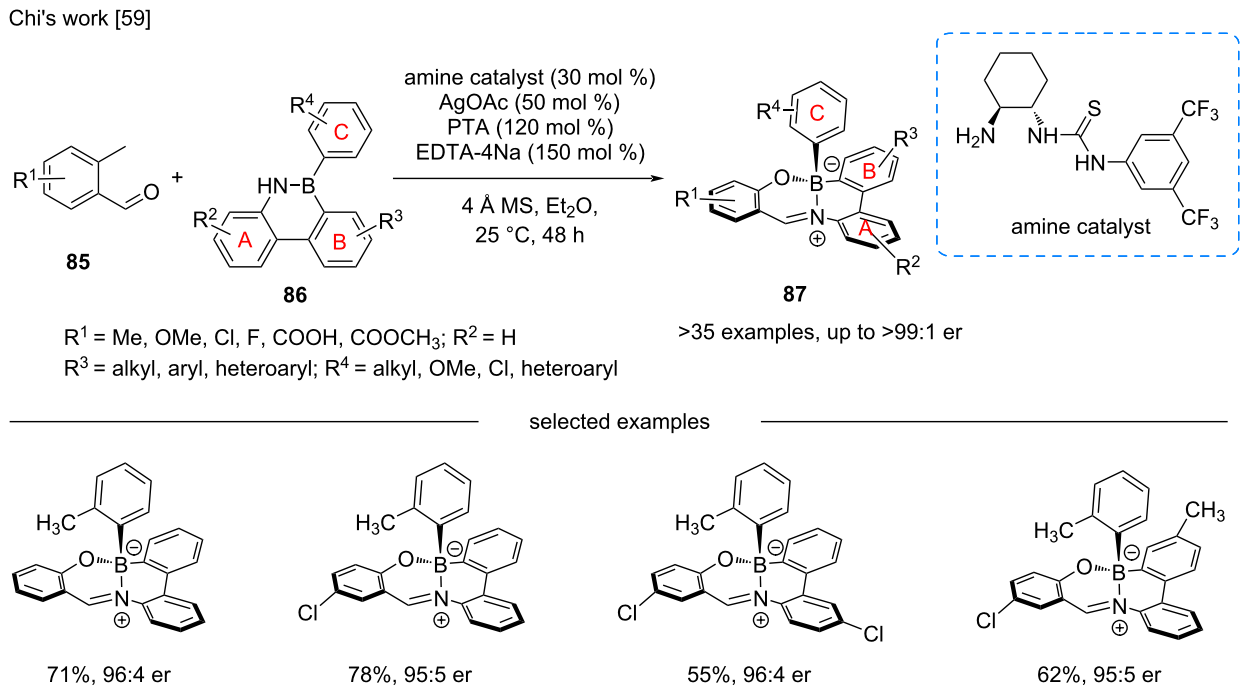
In 2025, Chi's group reported an unprecedented asymmetric B(sp^2)→B(sp^3) transformation enabled by amino thiourea organocatalysis coupled with iminium-ion activation, which allowed direct asymmetric addition to planar tricoordinate boron substrates (Scheme 23) [59]. This protocol enabled the streamlined one-step assembly of tetracoordinate boron-stereogenic heterocycles **87**, circumventing the conventional reliance on metal-catalyzed desymmetrization or prefunctionalized tetracoordinate boron precursors that dominate classic boron-stereogenic synthesis.

This transformation employs salicylaldehydes **85** and *B*,*N*-phenanthroline-based boron-containing aromatics **86** as substrates. The catalytic system is based on a chiral cyclohexanediamine-derived primary amine-thiourea bifunctional organocatalyst, assisted by silver acetate as co-catalyst and an alkaline buffer composed of EDTA-4Na and terephthalic acid. The low-polarity solvent diethyl ether effectively suppressed racemization side-reactions, and the overall dehydration and cyclization process was complete within 48 hours at ambient temperature.

In 2026, Song's group established a chiral phosphoric acid-catalyzed organocatalytic strategy for the construction of two unprecedented classes of tetracoordinate boron-stereogenic frameworks (Scheme 24) [60]. Using boron cyclohexanones **88** as common substrates, two distinct asymmetric transformations



Scheme 22: Synthesis of chiral boron BODIPYs via desymmetrization reactions catalyzed by N-heterocyclic carbene.



Scheme 23: Organocatalytic iminium-assisted asymmetric B(sp^2)-to-B(sp^3) transformation. PTA = *p*-phthalic acid.

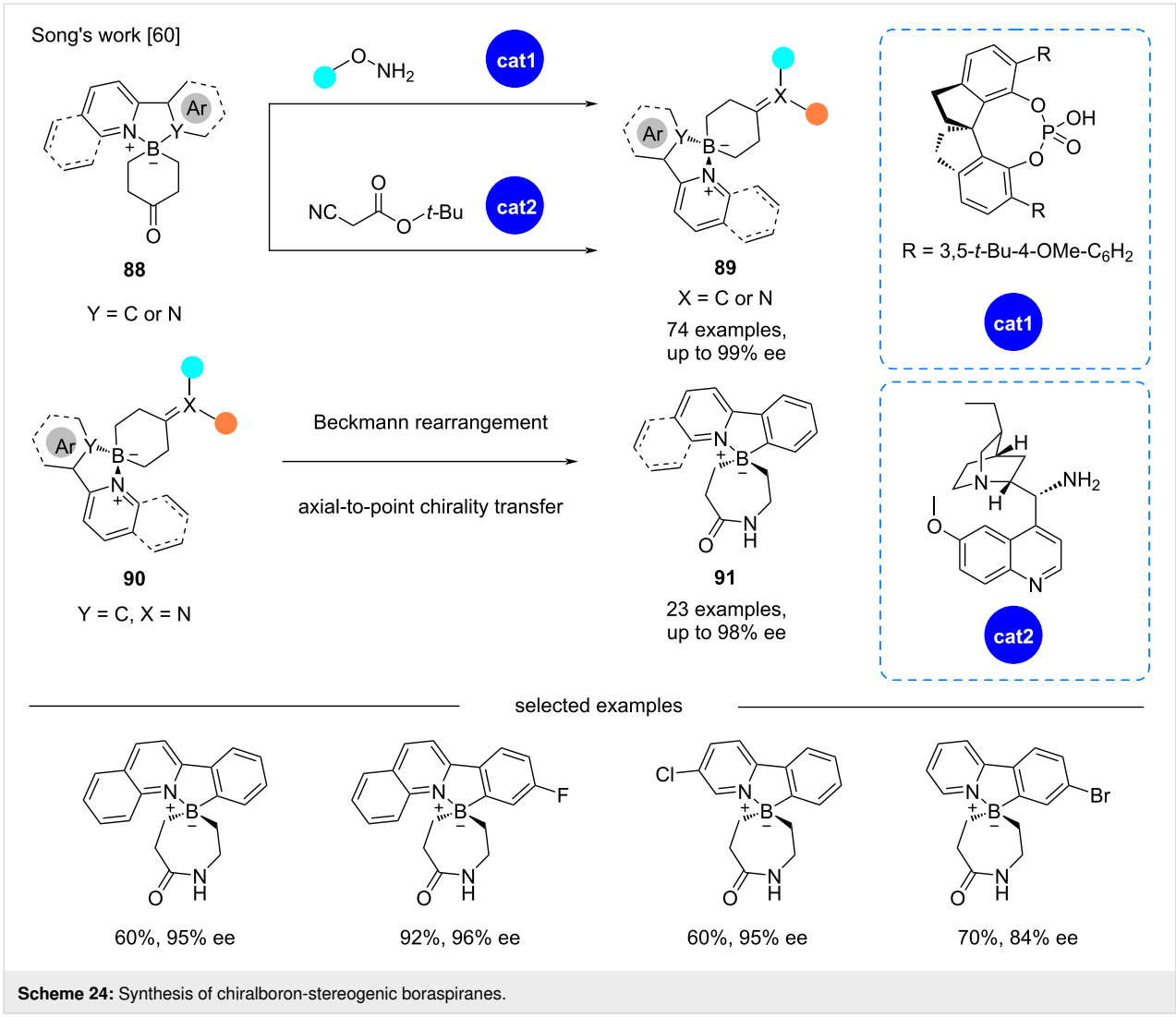
were developed. *O*-Arylhydroxylamines participated in the chiral phosphoric acid-catalyzed condensation to afford C=N-type axially chiral boracyclohexylidenes **89**, whereas *tert*-butyl cyanoacetate served as the reaction partner in an organocatalytic asymmetric Knoevenagel condensation to furnish C=C-type axially chiral boracyclohexylidenes **89**. The resulting axially chiral boron cyclohexyl scaffolds **90** served as versatile intermediates. Boron trichloride-promoted Beckmann rearrangement enables chirality transfer from axial chirality to boron-centered stereogenicity, affording the first class of boron-stereogenic boraspiranes **91** with a stereogenic boron center. The protocol exhibited excellent tolerance toward electronic and steric variations of substrate substituents, accommodating aryl, heteroaryl, and fused aromatic skeletons. The corresponding products were obtained in yields up to 98% and enantioselectivities as high as 99%.

Phase-transfer catalysis

In 2025, Hao's group disclosed a phase-transfer catalysis (PTC)-enabled enantioselective C–N coupling protocol (Scheme 25) [61]. This transformation employed α,α-dichloro-BODIPYs **92** and diverse nitrogen nucleophiles **93** (amides, carbamates, ureas, sulfonimides) as starting materials. Through nucleophilic aromatic substitution (S_NAr), the reaction efficiently furnished boron-stereogenic aminoamide-functionalized BODIPYs **94**. This work represents an innovative extension of phase-transfer catalysis to boron-stereogenic center construction. The protocol features mild reaction conditions, commercially accessible catalysts, broad functional-group tolerance, and a transition-metal-free nature.

In 2025, Jiang's group reported a phase-transfer-catalyzed (PTC) enantioselective C–N-bond-forming S_NAr reaction (Scheme 26) [62]. 3,5-Dihalogenated BODIPY **95** acted as the electrophilic substrate, with amides **96** serving as nucleophiles. Enantioselectivity was governed by the cooperative effect of a quinine-derived chiral phase-transfer catalyst and KOH, affording more than 40 previously unreported boron-stereogenic 3-amido-BODIPY derivatives **97**. This protocol delivered excellent yields of up to 99% alongside outstanding enantioselectivity with ee values reaching 99%. It features a broad substrate scope that accommodates arylamides, alkylamides, enoylamides, and heterocyclic amides with distinct electronic and steric properties.

In 2026, Li's group developed an asymmetric formal C(sp^2)–O/O–H metathesis reaction enabled by cinchona alkaloid-derived chiral quaternary ammonium salts (Scheme 27) [63]. Employing α,α-diaryloxy-BODIPYs **98** as the substrate and diverse alcohols **99** as nucleophiles, this protocol efficiently furnished boron-stereogenic BODIPY derivatives **100**. The transformation proceeded via a cooperative S_NAr pathway. The optimal catalytic system consisted of a naphthyl-functionalized cinchona quaternary ammonium salt with cesium carbonate in



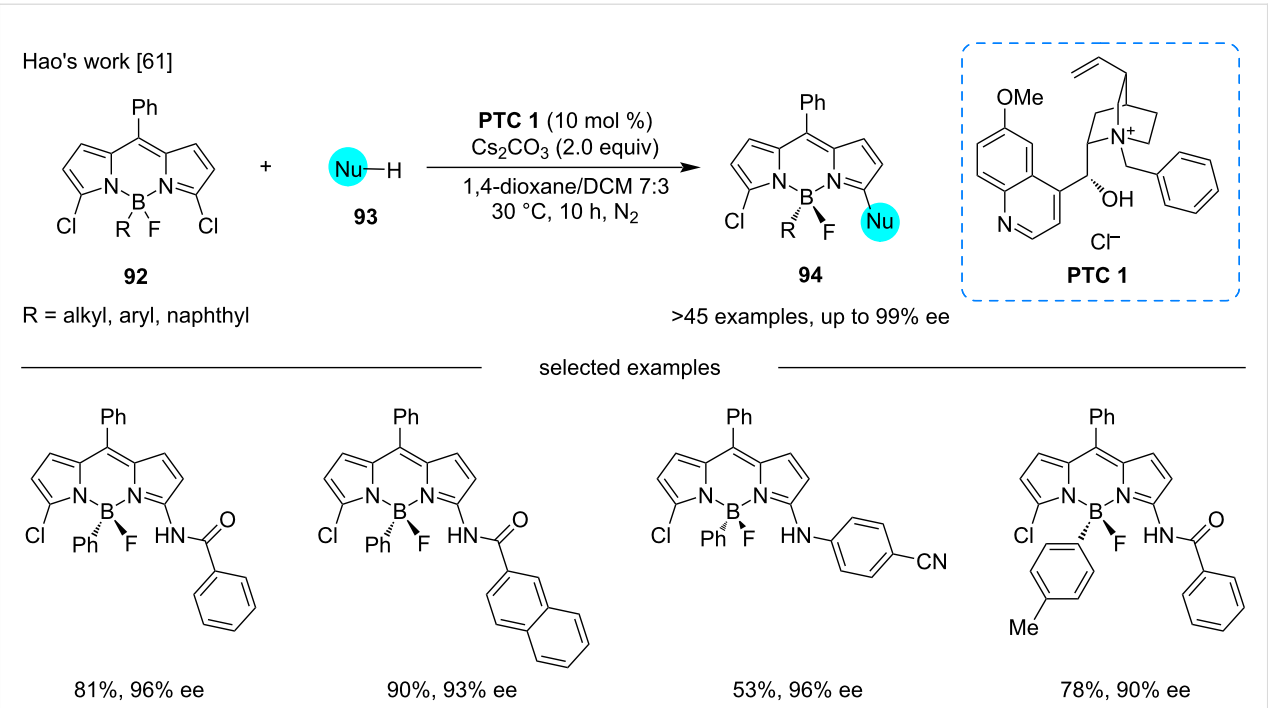
Scheme 24: Synthesis of chiralboron-stereogenic boraspiranes.

cold acetonitrile. Multiple hydrogen-bonding interactions and proton transfer among the catalyst, substrate, and alcohol nucleophile collectively govern the stereochemical outcome, providing a series of α,α-dialkoxy- and α,α-diaryloxy boron-stereogenic BODIPY products.

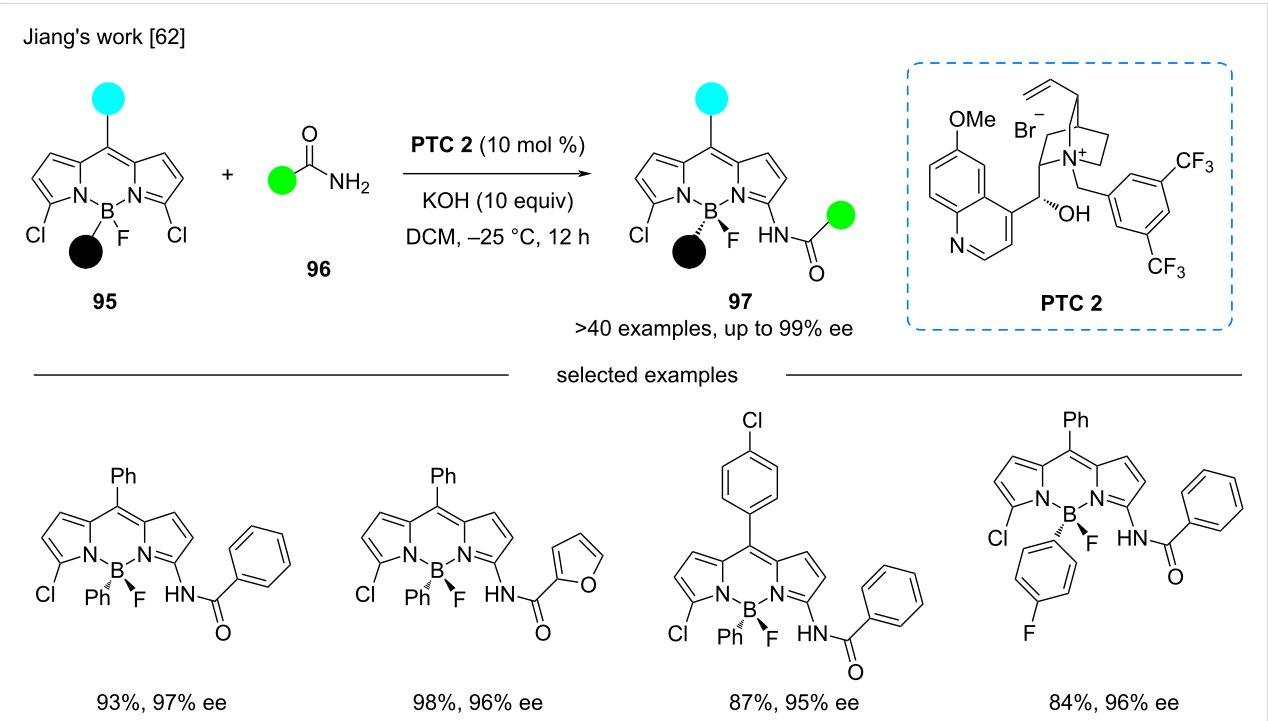
In 2026, Wang's group disclosed a biomimetic bisphosphonium salt-catalyzed asymmetric nucleophilic aromatic substitution (S_NAr) reaction for the highly enantioselective assembly of boron-stereogenic BODIPY scaffolds (Scheme 28) [64]. This protocol utilized prochiral α,α-dichloro-BODIPY **101** as the starting substrate, which undergoes desymmetrization with diverse phenolic oxygen nucleophiles **102**. Stepwise monosubstitution enabled the efficient synthesis of oxygen-functionalized boron-stereogenic BODIPY derivatives **103**. This study represents the first implementation of an amide-modified bisphosphonium salt catalytic system for the asymmetric fabrication of boron-stereogenic centers. The method features broad substrate generality, high yields up to 99%, and excellent enantioselectivity reaching 99% ee, while maintaining an entirely transition-metal-free process.

Comparison of synthetic strategies and future challenges

The development of catalytic asymmetric synthesis has significantly advanced the construction of boron-stereogenic tetracoordinate compounds. As discussed above, six major catalytic strategies have emerged, including copper-, palladium-, rhodium-, nickel/cobalt-, organocatalytic, and phase-transfer-catalytic approaches. Although these methods have enabled the efficient preparation of enantioenriched boron-stereogenic compounds, they differ considerably in their reaction modes, substrate compatibility, and stereochemical outcomes. A systematic comparison of their advantages and limitations is therefore essential for guiding the further development of this field.

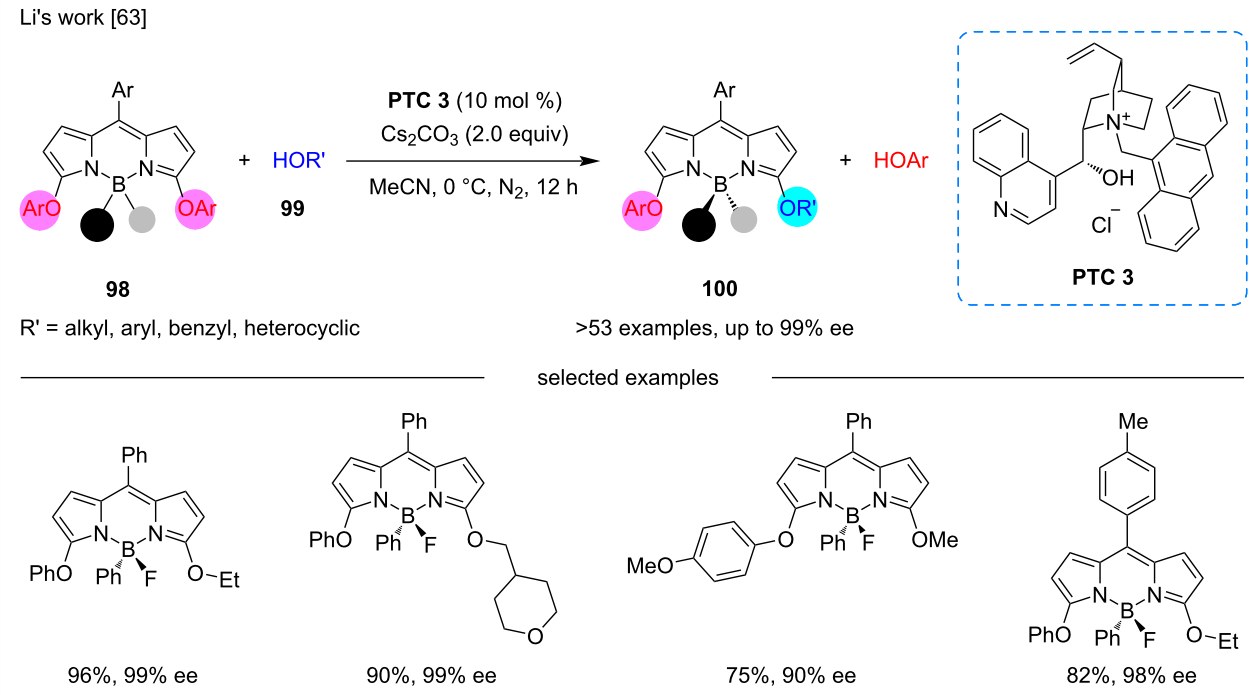


Scheme 25: Synthesis of boron chiral compounds via enantioselective carbon–nitrogen coupling reactions promoted by phase-transfer catalyst.

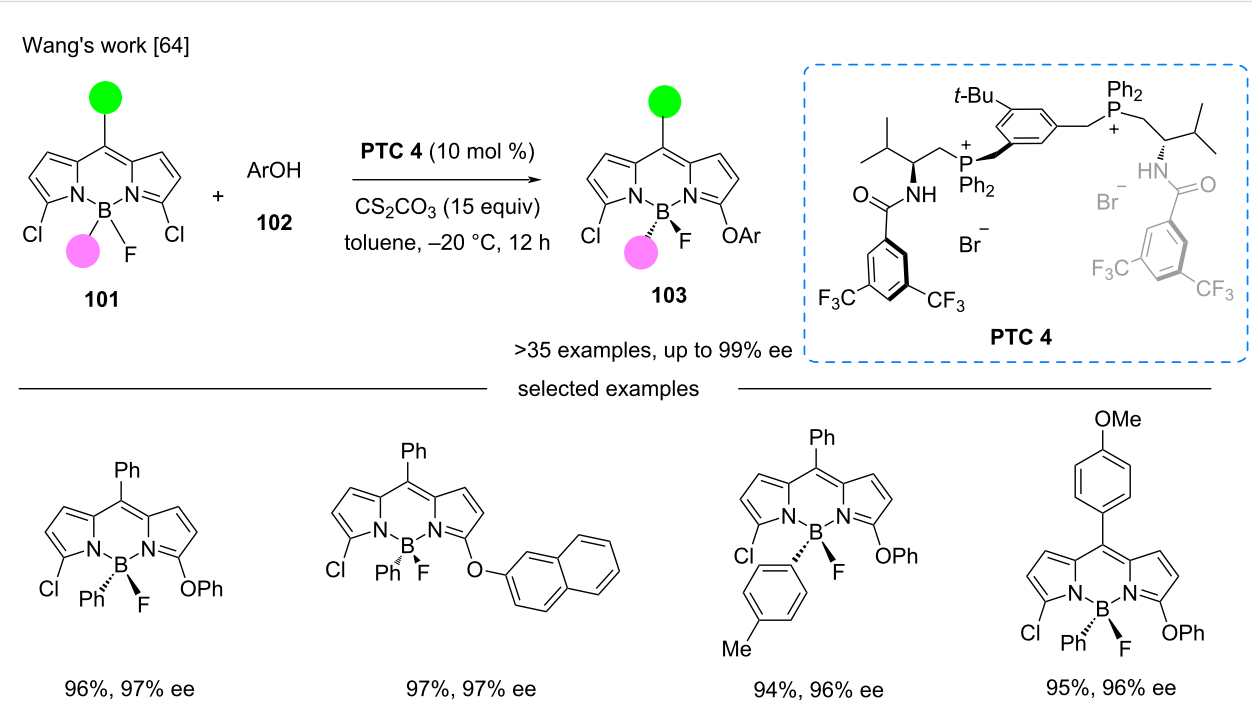


Scheme 26: Synthesis of boron-chiral compounds via asymmetric C–N-bond-forming S_NAr reaction mediated by phase-transfer catalysis.

Copper catalysis offers versatile approaches to the asymmetric construction of boron-stereogenic compounds through transformations such as azide–alkyne cycloaddition [39] and B–H carbene insertion [40,41]. These reactions can achieve high enantioselectivity and, in some cases, enable the simultaneous construction of adjacent boron- and carbon-stereogenic centers.



Scheme 27: Construction of boron-stereogenic BODIPYs through organo-catalyzed enantioselective formal C(sp^2)–O/O–H metathesis.



Scheme 28: Construction of boron-stereogenic BODIPYs via a bioinspired bisphosphonium salt-catalyzed S_NAr reaction.

However, their efficiency and stereoselectivity often depend on the compatibility of the substrate, chiral ligand, and reaction conditions.

Palladium catalysis is particularly useful for the asymmetric functionalization of BODIPY scaffolds through C–H arylation and coupling reactions [43-46], allowing modular structural

modification and access to functionalized chiral products. Its main limitation is the current emphasis on BODIPY-based substrates, highlighting the need to extend these methods to other boron frameworks.

Rhodium catalysis supports diverse transformations, including carbene insertion [48,49], C–H functionalization [50], and asymmetric cyclization [51], enabling the construction of complex boron-containing structures and multiple stereogenic elements. Nevertheless, stereocontrol can be sensitive to substrate structure and catalyst design, requiring further mechanistic investigation and broader substrate validation.

Nickel/cobalt catalysis expand the accessible molecular architectures through annulation [53], cycloaddition [54], hydroboration [55], and C–H activation [56]. These methods are especially promising for constructing spirocyclic frameworks and compounds containing multiple stereogenic elements. However, their substrate scope and functional-group compatibility remain to be explored more broadly.

Organocatalysis offers a transition-metal-free alternative and distinct approaches to stereogenic boron construction, including desymmetrization [58], kinetic resolution [57], direct $B(sp^2)$-to-$B(sp^3)$ conversion [59], and chirality transfer [60]. Its advantages include access to structurally diverse products and alternative modes of stereochemical induction. However, catalytic efficiency and enantioselectivity may be sensitive to substrate electronics, catalyst structure, and reaction conditions.

Phase-transfer catalysis (PTC) has emerged as an effective approach to the asymmetric functionalization of BODIPYs, particularly through C–N and C–O bond formation via nucleophilic aromatic substitution and related pathways [61-64]. Chiral phase-transfer catalysts facilitate reactions under transition-metal-free conditions, often with high yields, excellent enantioselectivity, and broad nucleophile compatibility. Nevertheless, current applications remain concentrated on BODIPY substrates, and further studies are needed to clarify catalyst–substrate interactions and extend the methodology to other boron-stereogenic frameworks.

Overall, each strategy offers distinct advantages, but no single method is universally applicable (Table 1). Future research should focus on expanding the substrate scope beyond established structural motifs, developing more general catalytic systems, and achieving more predictable stereocontrol. A deeper mechanistic understanding of catalyst–substrate interac-

Table 1: Advantages and limitations of the six synthetic strategies[a].

Synthetic strategy	main advantages	potential limitations
copper catalysis	offers diverse reaction types, including B–H-bond insertion, and enables the construction of multiple stereogenic centers with high enantioselectivity in selected cases	some reactions rely on specific substrate scaffolds and chiral ligands, and the substrate scope remains to be further expanded
palladium catalysis	particularly effective for selective functionalization of BODIPY scaffolds, enabling the construction of diverse boron-centered chiral structures	applications remain largely focused on BODIPY substrates; some transformations require prefunctionalized substrates and carefully optimized catalytic systems
rhodium catalysis	supports diverse transformations, including carbene insertion, C–H functionalization, and cyclization, and can construct adjacent boron- and carbon-stereogenic centers or additional chiral elements	the enantioselectivity of some reactions still has room for improvement, and substrate and ligand design have a substantial influence on the reaction outcome
nickel/cobalt catalysis	enables cyclization, cycloaddition, and the cooperative construction of boron-centered and other stereogenic elements	these methods remain at a relatively early stage of development; their generality, reaction mechanisms, and applicability to different substrates require further investigation
organocatalysis	provides transition-metal-free approaches and diverse reaction modes, including desymmetrization, kinetic resolution, direct $B(sp^2)\rightarrow B(sp^3)$ conversion, and chirality transfer	different reaction classes require distinct stereocontrol mechanisms; substrate scope, catalytic efficiency, and compatibility with varied reaction conditions remain important challenges
phase-transfer catalysis	enables asymmetric C–N and C–O-bond formation on BODIPY scaffolds under mild, transition-metal-free conditions, often with high yields and enantioselectivities	current applications are concentrated on BODIPY substrates and selected nucleophilic substitution pathways; broader scaffold compatibility and additional functionalization modes remain to be explored

[a]The limitations summarized above are based on the reaction types and substrate scope discussed in this review. They do not imply that every catalytic method has all the limitations listed.

tions, together with systematic investigations of racemization barriers and configurational stability, will be essential for designing robust boron-stereogenic compounds. Furthermore, improving synthetic scalability, operational simplicity, and catalyst accessibility, while exploring applications in asymmetric catalysis, pharmaceuticals, and functional materials, will be crucial for translating advances in asymmetric synthesis into practical utility.

Conclusion

In this review, we primarily summarized research progress reported up to 2026 on the asymmetric catalytic synthesis of enantioenriched boron-stereogenic compounds. Currently, the strategies can be categorized into six types: copper-, palladium-, rhodium-, nickel/cobalt-, organocatalytic, and phase-transfer-catalytic methods. In recent years, the enantioselective synthesis of chiral boron compounds has experienced vigorous development, yet it still faces significant challenges. At present, most methods rely on desymmetrization strategies, and we hope that more diverse approaches will be developed in the future, particularly to achieve precise stereocontrol over prochiral substrates. Meanwhile, current synthetic methodologies for chiral tetracoordinate boron compounds remain largely confined to academic study and are far from practical application. Nevertheless, we believe that continued research efforts will lead to further breakthroughs in both the synthesis and application of boron-stereogenic compounds.

Author Contributions

Yongke Wang: writing – original draft. Sichao Tian: supervision; writing – review & editing. Weidong Zhang: supervision; writing – review & editing.

ORCID® iDs

Yongke Wang - https://orcid.org/0009-0003-5833-3860

Data Availability Statement

Data sharing is not applicable as no new data was generated or analyzed in this study.

References

1. Yang, K.; Song, Q. *Acc. Chem. Res.* **2021,** *54,* 2298–2312. doi:10.1021/acs.accounts.1c00132
2. Schraff, S.; Sun, Y.; Pammer, F. *J. Mater. Chem. C* **2017,** *5,* 1730–1741. doi:10.1039/c6tc05418h
3. Abdou-Mohamed, A.; Aupic, C.; Fournet, C.; Parrain, J.-L.; Chouraqui, G.; Chuzel, O. *Chem. Soc. Rev.* **2023,** *52,* 4381–4391. doi:10.1039/d3cs00163f
4. Korobov, M. S.; Borodkin, G. S.; Borisenko, N. I.; Ryskina, T. A.; Nivorozhkin, L. E.; Minkin, V. I. *J. Mol. Struct.: THEOCHEM* **1989,** *200,* 61–72. doi:10.1016/0166-1280(89)85044-4
5. Braun, M. *Eur. J. Org. Chem.* **2024,** *27,* e202400052. doi:10.1002/ejoc.202400052
6. Guo, Y.; Zu, B.; Du Chen, C.; He, C. *Chin. J. Chem.* **2024,** *42,* 2401–2411. doi:10.1002/cjoc.202400130
7. Li, X.; Zhang, G.; Song, Q. *Chem. Commun.* **2023,** *59,* 3812–3820. doi:10.1039/d2cc06982b
8. Charoy, L.; Valleix, A.; Le Gall, T.; Pham van Chuong, P.; Mioskowski, C.; Toupet, L. *Chem. Commun.* **2000,** 2275–2276. doi:10.1039/b006265k
9. Toyota, S.; Hakamata, T.; Nitta, N.; Ito, F. *Chem. Lett.* **2004,** *33,* 206–207. doi:10.1246/cl.2004.206
10. Toyota, S.; Ito, F.; Nitta, N.; Hakamata, T. *Bull. Chem. Soc. Jpn.* **2004,** *77,* 2081–2088. doi:10.1246/bcsj.77.2081
11. Toyota, S.; Ito, F.; Yamamoto, T.; Akashi, H.; Iwanaga, T. *Bull. Chem. Soc. Jpn.* **2006,** *79,* 796–798. doi:10.1246/bcsj.79.796
12. Braun, M.; Schlecht, S.; Engelmann, M.; Frank, W.; Grimme, S. *Eur. J. Org. Chem.* **2008,** 5221–5225. doi:10.1002/ejoc.200800787
13. Jiménez, V. G.; Santos, F. M. F.; Castro-Fernández, S.; Cuerva, J. M.; Gois, P. M. P.; Pischel, U.; Campaña, A. G. *J. Org. Chem.* **2018,** *83,* 14057–14062. doi:10.1021/acs.joc.8b01844
14. Haefele, A.; Zedde, C.; Retailleau, P.; Ulrich, G.; Ziessel, R. *Org. Lett.* **2010,** *12,* 1672–1675. doi:10.1021/ol100109j
15. Gobo, Y.; Matsuoka, R.; Chiba, Y.; Nakamura, T.; Nabeshima, T. *Tetrahedron Lett.* **2018,** *59,* 4149–4152. doi:10.1016/j.tetlet.2018.10.003
16. Vedejs, E.; Fields, S. C.; Hayashi, R.; Hitchcock, S. R.; Powell, D. R.; Schrimpf, M. R. *J. Am. Chem. Soc.* **1999,** *121,* 2460–2470. doi:10.1021/ja983555r
17. Vedejs, E.; Fields, S. C.; Lin, S.; Schrimpf, M. R. *J. Org. Chem.* **1995,** *60,* 3028–3034. doi:10.1021/jo00115a017
18. Vedrenne, P.; Le Guen, V.; Toupet, L.; Le Gall, T.; Mioskowski, C. *J. Am. Chem. Soc.* **1999,** *121,* 1090–1091. doi:10.1021/ja983566k
19. Beltrán, H. I.; Zamudio-Rivera, L. S.; Mancilla, T.; Santillan, R.; Farfán, N. *J. Organomet. Chem.* **2002,** *657,* 194–204. doi:10.1016/s0022-328x(02)01418-3
20. Kaiser, P. F.; White, J. M.; Hutton, C. A. *J. Am. Chem. Soc.* **2008,** *130,* 16450–16451. doi:10.1021/ja8044629
21. Schlecht, S.; Frank, W.; Braun, M. *Eur. J. Org. Chem.* **2010,** 3721–3731. doi:10.1002/ejoc.201000406
22. Montalbano, F.; Candeias, N. R.; Veiros, L. F.; André, V.; Duarte, M. T.; Bronze, M. R.; Moreira, R.; Gois, P. M. P. *Org. Lett.* **2012,** *14,* 988–991. doi:10.1021/ol203224n
23. Flagstad, T.; Petersen, M. T.; Nielsen, T. E. *Angew. Chem., Int. Ed.* **2015,** *54,* 8395–8397. doi:10.1002/anie.201502989
24. Algoazy, N.; Knight, J. G.; Waddell, P. G.; Aerts, R.; Herrebout, W.; Al-Sharif, H. H. T.; Karlsson, J. K. G.; Harriman, A. *Chem. – Eur. J.* **2021,** *27,* 5246–5258. doi:10.1002/chem.202005246
25. Aupic, C.; Abdou Mohamed, A.; Figliola, C.; Nava, P.; Tuccio, B.; Chouraqui, G.; Parrain, J.-L.; Chuzel, O. *Chem. Sci.* **2019,** *10,* 6524–6530. doi:10.1039/c9sc01454c
26. Stöckl, Y.; Tait, E. J.; Frey, W.; Wegner, S.; Claasen, B.; Zens, A.; Laschat, S. *Chem. – Eur. J.* **2023,** *29,* e202301324. doi:10.1002/chem.202301324
27. Ray, C.; Avellanal-Zaballa, E.; Muñoz-Úbeda, M.; Colligan, J.; Moreno, F.; Muller, G.; López-Montero, I.; Bañuelos, J.; Maroto, B. L.; de la Moya, S. *Org. Chem. Front.* **2023,** *10,* 5834–5842. doi:10.1039/d3qo01561k
28. Ryschkewitsch, G. E.; Garrett, J. M. *J. Am. Chem. Soc.* **1968,** *90,* 7234–7238. doi:10.1021/ja01028a011

29. Imamoto, T.; Morishita, H. *J. Am. Chem. Soc.* **2000,** *122,* 6329–6330. doi:10.1021/ja0011764
30. Beltrán, H. I.; Alas, S. J.; Santillan, R.; Farfán, N. *Can. J. Chem.* **2002,** *80,* 801–812. doi:10.1139/v02-109
31. Montalbano, F.; Cal, P. M. S. D.; Carvalho, M. A. B. R.; Gonçalves, L. M.; Lucas, S. D.; Guedes, R. C.; Veiros, L. F.; Moreira, R.; Gois, P. M. P. *Org. Biomol. Chem.* **2013,** *11,* 4465–4472. doi:10.1039/c3ob40614h
32. Montalbano, F.; Leandro, J.; Farias, G. D. V. F.; Lino, P. R.; Guedes, R. C.; Vicente, J. B.; Leandro, P.; Gois, P. M. P. *RSC Adv.* **2014,** *4,* 61022–61027. doi:10.1039/c4ra10306h
33. Faustino, H.; Silva, M. J. S. A.; Veiros, L. F.; Bernardes, G. J. L.; Gois, P. M. P. *Chem. Sci.* **2016,** *7,* 5052–5058. doi:10.1039/c6sc01520d
34. Vedejs, E.; Chapman, R. W.; Fields, S. C.; Lin, S.; Schrimpf, M. R. *J. Org. Chem.* **1995,** *60,* 3020–3027. doi:10.1021/jo00115a016
35. Maeda, C.; Nagahata, K.; Shirakawa, T.; Ema, T. *Angew. Chem., Int. Ed.* **2020,** *59,* 7813–7817. doi:10.1002/anie.202001186
36. Uraguchi, D.; Ueoka, F.; Tanaka, N.; Kizu, T.; Takahashi, W.; Ooi, T. *Angew. Chem., Int. Ed.* **2020,** *59,* 11456–11461. doi:10.1002/anie.202001637
37. Zhao, L.; Zhou, H.; Zhou, Q.; Peng, C.; Cheng, T.; Liu, G. *Sens. Actuators, B* **2020,** *320,* 128383. doi:10.1016/j.snb.2020.128383
38. Zhao, J.; Ren, L.-Q.; Lan, D.; Zhan, B.; Zhang, J.; Mu, J.; He, C. *Nat. Commun.* **2025,** *16,* 9719. doi:10.1038/s41467-025-64709-z
39. Zu, B.; Guo, Y.; He, C. *J. Am. Chem. Soc.* **2021,** *143,* 16302–16310. doi:10.1021/jacs.1c08482
40. Zhang, G.; Zhang, Z.; Hou, M.; Cai, X.; Yang, K.; Yu, P.; Song, Q. *Nat. Commun.* **2022,** *13,* 2624. doi:10.1038/s41467-022-30287-7
41. Zhang, G.; Cai, X.; Jia, J.; Feng, B.; Yang, K.; Song, Q. *ACS Catal.* **2023,** *13,* 9502–9508. doi:10.1021/acscatal.3c02093
42. Zhang, G.; Jia, J.; Du, X.; Feng, B.; Yang, K.; Yu, P.; Song, Q. *Nat. Commun.* **2025,** *16,* 9955. doi:10.1038/s41467-025-64905-x
43. Zu, B.; Guo, Y.; Ren, L.-Q.; Li, Y.; He, C. *Nat. Synth.* **2023,** *2,* 564–571. doi:10.1038/s44160-023-00262-1
44. Ren, L.-Q.; Zhan, B.; Zhao, J.; Guo, Y.; Zu, B.; Li, Y.; He, C. *Nat. Chem.* **2025,** *17,* 83–91. doi:10.1038/s41557-024-01649-z
45. Kondo, A.; Takano, H.; Shinokubo, H. *Chem. Lett.* **2025,** *54,* upae218. doi:10.1093/chemle/upae218
46. Zhan, B.; Ren, L.-Q.; Zhao, J.; Zhang, H.; He, C. *Nat. Commun.* **2025,** *16,* 438. doi:10.1038/s41467-024-55796-5
47. Li, L.; Gong, X.; Kou, Z.; Yan, Q.; Ji, X.; Luan, X.; Nan, J. *J. Am. Chem. Soc.* **2026,** *148,* 25258–25268. doi:10.1021/jacs.6c08339
48. Ankudinov, N. M.; Komarova, A. A.; Podyacheva, E. S.; Chusov, D. A.; Danshina, A. A.; Perekalin, D. S. *Chem. Commun.* **2024,** *60,* 8601–8604. doi:10.1039/d4cc02969k
49. Ankudinov, N. M.; Alexeev, N. V.; Podyacheva, E. S.; Chusov, D. A.; Lyssenko, K. A.; Perekalin, D. S. *Chem. Sci.* **2025,** *16,* 6298–6306. doi:10.1039/d5sc00723b
50. Gao, Y.; Liu, Z.; Tian, S.; Min, Y.; Li, X.; Chen, Y.; Hong, X.; Zhang, W.; Wang, L. *Angew. Chem., Int. Ed.* **2025,** *64,* e202418888. doi:10.1002/anie.202418888
51. Zhu, X.; Shi, Y.; Li, J.; Peng, H.; Gong, M.; Zhou, W.; Wang, F.; Huang, G.; Li, X.; Fang, Y. *Nat. Commun.* **2025,** *16,* 9764. doi:10.1038/s41467-025-64698-z
52. Liu, J.-G.; Zhang, W.-P.; Xu, M.-H. *J. Am. Chem. Soc.* **2025,** *147,* 33691–33699. doi:10.1021/jacs.5c09400
53. Ma, B.; Tang, X.; Zhou, X.; Meng, D.; Feng, A.; Qian, D. *Org. Lett.* **2025,** *27,* 14100–14106. doi:10.1021/acs.orglett.5c04722
54. Cao, Y.-X.; Chauvin, A.-S.; Tong, S.; Alama, L.; Cramer, N. *Nat. Catal.* **2025,** *8,* 569–578. doi:10.1038/s41929-025-01352-3
55. Fang, S.; Zhang, P.; Hu, G.; Lyu, H.; Quan, Y. *J. Am. Chem. Soc.* **2026,** *148,* 12166–12175. doi:10.1021/jacs.6c00475
56. Yang, T.; Han, S.; Meng, X.; Dou, Y.; Yang, D.; Niu, J.-L. *J. Am. Chem. Soc.* **2026,** *148,* 18882–18894. doi:10.1021/jacs.6c00543
57. Gao, Y.-Y.; Liang, Y.-J.; Li, G.; Li, L.; Hu, Z.-Y.; Lin, W.-H.; Huang, X.-H.; Chen, Y.; Du, X.; Yu, P.; Song, Q.; Liu, L. *ACS Catal.* **2025,** *15,* 9346–9352. doi:10.1021/acscatal.5c01629
58. Ma, J.; Guo, L.; Zhang, X.-Q.; Tang, W.-W.; Guo, X.; Kang, Z.; Jiao, L.; Hao, E.; Li, Z.-Y. *JACS Au* **2025,** *5,* 2837–2848. doi:10.1021/jacsau.5c00425
59. Nong, Y.; Vummaleti, S. V. C.; Zhang, Y.; Sun, Y.; Chen, L.; Jin, Z.; Huang, H.; Hao, E.; Zhang, X.; Chi, Y. R. *Nat. Commun.* **2025,** *16,* 10452. doi:10.1038/s41467-025-65393-9
60. Wang, S.; Liu, J.; Li, W.; Li, Y.; Huang, Y.; Ma, W.; Song, Q. *Chem* **2026,** *12,* 102990. doi:10.1016/j.chempr.2026.102990
61. Zhang, X.-Q.; Lv, X.-J.; Guo, L.; Ma, J.; Su, B.; Hu, Y.; Jiao, L.; Li, Z.-Y.; Hao, E. *Nat. Commun.* **2025,** *16,* 2735. doi:10.1038/s41467-025-58117-6
62. Meng, Y.-D.; Fang, W.; Pei, Z.-H.; Chen, W.-H.; Ding, S.-Y.; Shen, M.-L.; Bu, Y.; Yao, C.-Z.; Li, Q.; Yu, J.; Jiang, H.-J. *JACS Au* **2025,** *5,* 1965–1973. doi:10.1021/jacsau.5c00196
63. Zhang, J.-L.; Ma, J.; Guo, L.; Hu, Y.; Huang, S.; Hao, E.; Li, Z.-Y. *Nat. Commun.* **2026,** *17,* 6308. doi:10.1038/s41467-026-72860-4
64. Yang, Q.; Wu, J.-H.; Ma, J.; Liu, Z.; Yang, C.; Fang, S.; Wang, T. *ACS Catal.* **2026,** *16,* 16393–16402. doi:10.1021/acscatal.6c05079

License and Terms

This is an open access article licensed under the terms of the Beilstein-Institut Open Access License Agreement (https://www.beilstein-journals.org/bjoc/terms), which is identical to the Creative Commons Attribution 4.0 International License (https://creativecommons.org/licenses/by/4.0). The reuse of material under this license requires that the author(s), source and license are credited. Third-party material in this article could be subject to other licenses (typically indicated in the credit line), and in this case, users are required to obtain permission from the license holder to reuse the material.

The definitive version of this article is the electronic one which can be found at:
https://doi.org/10.3762/bjoc.22.139